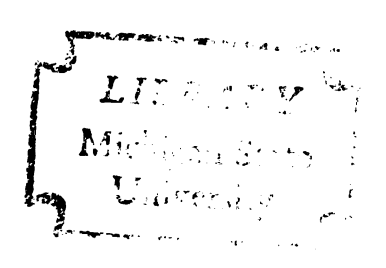
A KINETIC MODEL FOR THE REACTIONS OF CO AND H2 TO CH4 AND C2H2 IN A FLOW MICROWAVE PLASMA REACTOR

Thesis for the Degree of M. S. MICHIGAN STATE UNIVERSITY STEVEN F. MERTZ
1975

THESIS





ABSTRACT

A KINETIC MODEL FOR THE REACTIONS OF CO AND $\rm H_2$ TO $\rm CH_4$ AND $\rm C_2H_2$ IN A FLOW MICROWAVE DISCHARGE REACTOR

By

Steven F. Mertz

A kinetic model was developed to describe the reactions of CO and H_2 to CH_4 and C_2H_2 in a microwave plasma. The experimental system consisted of a 24 mm I.D. tubular quartz reactor which passed through a microwave cavity. A variable-incident power waveguide system could supply up to 800 watts of incident microwave power to the cavity. The reactant gas mixture of H2 and CO flowed through the reactor, where a plasma was maintained under pressures of 20-100 mm Hg. The reactor effluent was analyzed by IR spectroscopy for CH_4 and C_2H_2 . Conversions of up to 5.3% CO to C_2H_2 and 7.2% CO to CH_4 were observed. A 26-reaction kinetic model was developed and fitted to the experimental data. The plasma reactor was modeled in two zones: a discharge zone where electron-impact dissociations produce H, C, and O, and a downstream recombination zone where the atomic species from the discharge recombine. discharge zone was modeled as a well-mixed reactor, and the recombination zone was modeled as a plug-flow reactor. The model was able to explain the asympotic shape of the observed conversion versus residence time data; the effect is due to a kinetic limitation. This also explains why the conversions obtained in the plasma cannot be predicted by thermodynamic equilibrium.

a kinetic model for the reactions of co and $\rm H_2$ to $\rm CH_4$ and $\rm C_2H_2$ in a flow microwave plasma reactor

by

Steven F. Mertz

A THESIS

Submitted to

Michigan State University
in partial fulfillment of the requirements
for the degree of

MASTER OF SCIENCE

Department of Chemical Engineering

1975

ACKNOWLEDGEMENT

The author gratefully acknowledges the Detroit Edison Company and the Division of Engineering Research for their financial support of this project.

Sincere appreciation is extended to Dr. Martin C. Hawley and Dr. Jes Asmussen for their assistance and guidance during the course of this effort.

TABLE OF CONTENTS

I	Page
ABSTRACT	i
ACKNOWLEDGEMENTS	ii
INTRODUCTION	1
REVIEW OF PREVIOUS WORK	2
DESCRIPTION OF EXPERIMENTAL PROGRAM	6
Reactor Flow System	6
Plasma Cavity and Microwave System	6
Experimental Procedure	7
Experimental Results	7
DISCUSSION AND MODELING	11
Reactions of the H ₂ /CO Plasma System	11
Reactor Model	13
a) Plasma Zone	13
b) Recombination Zone	15
Data Fitting	16
Comparison of Model to Experimental Results	17
CONCLUSIONS	20
	-
NOTATION	21
REFERENCES	38
APPENDIX	41
Fortran Listing of Regression Program and	
Simplified Reactor Model	42
Fortran Listing of Complete Reactor Model	57
Suggestions for Future Work	66
Daggerous for Larate Mory	00

LIST OF FIGURES

- 1. Plasma Reactor Flow System
- 2. Plasma Cavity
- 3. Effect of Space Time on Conversion of ${\rm CO}$ to ${\rm CH}_4$
- 4. Effect of Space Time on Conversion of CO to C2H2
- 5. Effect of Pressure on Conversion of CO to CH₄ and C₂H₂
- 6. Effect of 6/1 and 2/1 H_2/CO Feeds on Conversion to CH_4
- 7. Effect of 6/1 and 2/1 H_2^-/CO Feeds on Conversion to $C_2^-H_2^-$
- 8. Effect of Pressure on Shape of Plasma
- 9. Conceptual Model of Plasma Reactor
- 10. Effect of Residence Time upon Concentration of Atomic Species Leaving Discharge
- 11. Concentration Profiles of Intermediates and Products in Recombination Zone

LIST OF TABLES

- 1. Reactions of H_2/CO Plasma System
- 2. Reactions Used in Simplified Model
- 3. Rate Expressions Used in Recombination Zone
- 4. Comparison of Literature Estimates of Rates to Rates from Regression

INTRODUCTION

Several investigators have successfully modeled discharge reactor systems for relatively simple reacting gas mixtures. Brown and Bell have studied the reactions of an O₂/CO/CO₂ discharge; Bell has modeled H₂ dissociation-recombination reactions; and Mearns and Morris have analyzed O₂ dissociation-recombination reactions. These investigators have simulated the behavior of simple reacting chemical systems using straightforward plug flow, backmix, and nonflow kinetic models. Their studies have defined the kinetic, discharge, and transport parameters that determine the chemical nature of plasma systems and have shown that such systems can be successfully described by kinetic models based on electron-impact dissociation and free radical recombination.

The objective of the work described in this paper was to extend the previous work in plasma kinetic modeling to complex systems involving multiple parallel and consecutive free radical reactions. The papers of Brown and Bell formed the groundwork for our investigation of the reactions of H_2 and CO to hydrocarbons in a microwave plasma system. The kinetic constants for H_2 and CO dissociation-recombination processes in discharges were determined from their experimental studies. A flow-reactor model for H_2 /CO plasmas was developed by combining the electron-impact dissociation-recombination kinetics of H_2 and CO plasmas with the recombination kinetics of hydrogen, carbon and hydrocarbon radicals. This model was successfully fitted to experimental data. This paper describes the experimental plasma system and experimental procedure, develops a kinetic model for analyzing plasma reactions, and reports the kinetic parameters used to fit the data.

The success of this model shows that the kinetic models of Bell and Brown can be extended to more complex reaction systems, and that plasma chemical reactions can be analyzed in terms of the kinetics of electron-impact dissociations and free radical recombinations.

PREVIOUS WORK

In addition to the kinetic modeling of Bell and Brown, a number of researchers have experimentally investigated carbon-hydrogen discharge systems. Baddour and Blanchet have studied the reactions of carbon vapor with hydrogen and methane. The carbon vapor was produced from the graphite electrodes of a 30 kw arc at atmospheric pressure. The temperature of this arc was estimated to be 3500-4500°K. By withdrawing gas from the arc through a water-cooled quench probe, mixtures of up to 26% acetylene in hydrogen could be obtained. Equilibrium calculations indicate that the maximum concentration of acetylene should be about 7%; however, it was explained that the high yield was due to the quench step.

Blaustein and Fu⁵ have studied the reaction of $\rm H_2/CO$ and $\rm H_2/CO_2$ mixtures in a nonflow 2450 MHz discharge reactor. Pressures of 12 and 50 torr and reaction times of 30 to 240 seconds were used. Without quenching, the maximum hydrocarbon yield was 17-18% conversion of CO to $\rm CH_4$ and $\rm C_2H_2$ at 12 torr, and 24-25% at 50 torr. By freezing out the water formed during the reaction, the conversion was increased to 78%. With a liquid $\rm N_2$ cold trap which froze out all the hydrocarbon products, conversions of about 90% were observed. The predominant products are $\rm CH_4$, $\rm C_2H_2$, and $\rm C_2H_6$; the ratio of products depends upon quench temperature. Very little $\rm C_2H_4$ was observed.

Lett, et. al., ⁶ have studied the reactions of an $H_2/CO/Ar$ mixture in a flow plasma system. A 2450 MHz microwave source was used. Mass spectrometry was used to analyze for hydrocarbon products. The major products were CH_4 and C_2H_2 ; negligible amounts of C_2H_4 and C_2H_6 were observed. The reaction appeared to have a first-order dependence upon CO concentration.

Baddour and Iwasyk have also reported the results of C/H_2 reactions in a high-intensity arc. As in the paper by Baddour and Blanchet, they have used an equilibrium approach to explain the formation of C_2H_2 in high-temperature systems; methane formation is not considered. A key reaction step in Baddour's analysis is the formation of C_2 radicals in the gas phase as a precursor of acetylene:

$$2C \rightarrow C_2$$

$$C_2 + H_2 \rightarrow C_2H_2$$

McTaggert⁸ and Vastola et. al. ⁹ have investigated low pressure reactions of H_2 , graphite, and CO in microwave (2450 MHz) flow reactors with low residence times. Only traces of hydrocarbon products (mainly CH_4 and C_2H_2) were observed in the gas collected from the H_2/CO discharge. A hydrogen conversion of about 10% was observed when graphite rods were suspended in a hydrogen discharge. Spectroscopic evidence indicates that CH radicals are intermediates in the formation of hydrocarbons.

Fu, Blaustein, and Wender $^{10, 11}$ have conducted pyrolysis experiments by heating coal in Ar, CO_2 , and H_2 discharges. The main products were H_2 , CO, and CO_2 . Some methane and acetylene were also produced.

A number of papers also deal with the kinetic analysis of plasma reactions. Kondratiev, et. al. ¹² have discussed the difficulties involved in calculating rate constants for plasma reactions from collision cross sections. Furthermore, there are problems associated with applying kinetic rates determined for molecules in the ground state to plasma reactions; while a large fraction of the molecules in a low-temperature plasma are not ionized or dissociated, it is likely that a significant number of these molecules will possess some excitation due to electron-molecule collisions. The deviation between the rate constants for excited molecules and for ground-state molecules can vary by 30 percent in some cases. Therefore, although the general principles of kinetic analysis apply to plasma reactions, the rate constants for plasma systems may vary from those measured for non-plasma gas phase reactions.

Polak 13 has observed that one of the main difficulties in relating kinetic data to theory for plasma systems is that low-temperature plasmas are not in thermal equilibrium. The activated complex theory of gas-phase reactions assumes an equilibrium between reactant molecules and the excited activated complex (which has a fixed probability of either proceeding to products or reverting to reactant

molecules); the Arrhenius equation for rate variation with temperature is a result of this theory. However, the reacting mixture must be in thermal equilibrium (i.e., have a Maxwell-Boltzman distribution of energies) in order to apply the activated complex theory. Hence, the temperature-rate variation for plasma reactions may not be adequately described by the Arrhenius equation. In order to rigorously treat low-temperature plasma processes, it is necessary to deal with several different temperatures: electron temperatures, ion temperatures, gas translational temperatures, gas rotational temperatures, and gas vibrational temperatures.

Polak has also developed a kinetic model for a high temperature plasma arc converting methane to acetylene. This system, which operates at a pressure of 1 atmosphere, probably approaches thermal equilibrium due to the high frequency of electron-gas collisions (due, in turn, to the high pressure). A classical multiple-reaction kinetic model using Arrhenius rates successfully described the performance of the plasma jet.

Bell and others ^{1, 2, 3, 14} have successfully modeled dissociation-recombination reactions in plasma systems. Bell has developed a general model for plasma reactions ¹⁴ that includes equations of continuity for electrons, ions, and uncharged species (free radicals and ground state molecules). He has applied this model to a hydrogen plasma ² for nonflow, backmix flow, and plug flow systems. Bell found that data for H₂ dissociation in a flowing microwave discharge was best described by a backmix model.

Bell and Brown have modeled the discharge reactions of CO and O_2 and the decomposition of CO_2 using a 15-reaction model. Their data were generated in a 13.56 MHz RF discharge; pressure varied from 2-32 torr, flow rate varied from 2-30 μ moles/sec., and power varied from 50-350 watts. Their model consisted of two plug flow reaction zones in series. In the first zone, electron impact dissociations form the reactive precursors of the products; in the second zone, these free radicals recombine to yield the final stable products. A correction was included for gas bypassing the plasma without reacting.

Bell and Kwong 15, 16 and Mearns and Morris have studied the dissociation-recombination reactions of oxygen discharges. Their

experiments were performed in flow reactors using either radio frequency or microwave excitation. The proposed reaction mechanism consists of electron impact dissociation followed by four competing recombination reactions. The important variables in plasma systems were reported to be gas flow rate, power, and pressure.

EXPERIMENTAL PROGRAM

A. Reactor Flow System

The plasma reactor flow system is shown in Figure 1. The reactor was a 24mm ID quartz tube passing through the axis of a cylindrical microwave cavity. The reactor could be operated at pressures from 2-100 torr. The quartz tube was cooled by an air stream directed into the cavity.

The reactor feed system consisted of a feed cylinder, flow meter, and feed valve. H₂ and CO were premixed at the desired feed ratio and stored in the feed cylinder during each series of experiments. A pressure regulator delivered the H₂/CO mixture to the rotameter at a constant pressure of 5 psig. The feed valve controlled the flow rate through the rotameter and throttled the feed to the reactor pressure.

The effluent from the reactor was passed through a 10-meter Perkin-Elmer gas IR cell for analysis. A silica-gel drying tube ahead of the IR cell removed any H_2O generated by the reactions; the IR absorption of water would otherwise mask the absorptions of CH_4 and C_2H_2 . After passing through the IR cell, the gases passed through another valve which was used to regulate the reactor pressure. The gases were then exhausted to vacuum.

B. Plasma Cavity and Microwave System

The plasma is generated within the cavity and is contained by the 24 mm ID quartz tube located along the axis of the cavity (Figure 2). The cavity has an I.D. of 20.3 cm and can be adjusted to a maximum length of 35 cm. The cavity is water cooled by externally soldered tubing coils. The quartz tube itself is cooled by an air blast directed into the cavity. The plasma can be viewed through a screened window in the cavity side wall.

The cavity is designed to operate in a number of different modes. Depending on the method of coupling energy into the cavity and the cavity length, either the TE* 112 or the TM 011 mode can be excited. A probe coupling is used to excite the TE* 112 mode, and a loop coupling is used to excite the TM 011 mode. The cavity length can also be adjusted to achieve maximum power absorption by the plasma. The optimum cavity length depends upon the cavity mode and the plasma pressure. During

the experiments described in this paper, the cavity was operated in the TE* 112 mode with a cavity length of 12-13 cm.

Power is coupled into the cavity from a variable-incident-power 2450 MHz microwave system. The maximum incident power is 800 watts. Power meters monitor the incident and reflected power; the difference between the two powers represents the power absorbed by the plasma. The cavity and power system were described in detail in earlier papers. 19, 20

C. Experimental Procedure

Prior to operating the system, the feed tank was evacuated and filled with H_2 and CO in a predetermined ratio. The reactor system was then evacuated. The plasma was ignited, and then the feed rate, reactor pressure, and absorbed power were adjusted to the desired levels. The system was allowed to operate for several minutes to guarantee that the IR cell was filled with steady-state reactor effluent, then the IR spectrum was scanned for CH_4 and C_2H_2 .

The concentrations of CH_4 and C_2H_2 in the reactor effluent were determined from the strength of their IR absorptions. The areas under the CH_4 absorption at 3000 cm⁻¹ and under the C_2H_2 absorption at 1300-1400 cm⁻¹ were compared to the areas obtained for mixtures of CH_4 and C_2H_2 in H_2 and C0 at concentrations corresponding to 5 and 10% conversion, and at the pressures of the experimental runs. The IR system was capable of detecting CH_4 and C_2H_2 concentrations as low as 0.05% at pressures above 20 mm Hg. No absorptions were observed for other hydrocarbons such as C_2H_4 and C_2H_6 , although mass spectroscopy indicated that they were present in small amounts.

D. Experimental Results

Our experimental program was designed to determine the effects of residence time, feed composition, pressure, and power on the conversion of CO and H₂ to hydrocarbons. Figures 3-7 show typical experimental results and will be compared to the results of the kinetic model described in the next section. A complete summary of the experimental results has been reported. ²⁰

Figures 3 and 4 show the effect of residence time on conversion.

The space time reported in these figures is defined as

$$\tau = \frac{V}{V}$$

where V_p is the observed plasma volume, and v_o is the volumetric flow of gas into the plasma zone. Due to the volumetric expansion that accompanies the partial dissociation of the reactant gases, the actual residence time is slightly less than the space time.

As can be seen, the conversion increases rapidly at first, but then asymptotically approaches a limiting conversion of about 7.3 percent to CH_4 and 5.3 percent to C_2H_2 . It should be noted that the total conversion of CO is the sum of the conversions shown in Figures 3 and 4, since both CH_4 and C_2H_2 are produced simultaneously.

Figure 5 illustrates the effect of plasma pressure on conversion. The data shown was taken at constant space time. As can be seen, for pressures above 20 mm Hg, conversion decreases as pressure increases.

Figures 6 and 7 show the effect of variation in feed composition. As expected, a large increase in the $\rm H_2/CO$ ratio increases the conversion of CO to hydrocarbons. The yield of $\rm C_2H_2$ shows some dependence upon power level (increasing the power level increases the conversion to $\rm C_2H_2$), but the conversion to $\rm CH_4$ does not depend strongly on the power level.

During the experiments, the plasma was observed to decrease in size as the pressure was increased. At high pressures the plasma was not symetrical; rather than being cylindrical or spherical, it appeared to be somewhat flattened (Figure 8). At pressures below 40 mm Hg, the plasma appeared to extend to the tube walls. At pressures above 40 mm, the plasma did not extend to the tube walls. At pressures of 80-100 mm, the plasma zone is a flattened sphere about 1.5 cm across. Because of the small size of the plasma zone, considerable bypassing occurs at high pressure.

During high pressure operation, a soft black deposit resembling soot appeared on the tube wall for a short distance immediately downstream and upstream of the plasma zone. This deposit apparently is due to the migration of carbon atoms to the tube wall, where they condense to form an amorphous carbon deposit. The tube wall is subject to severe local heating around carbon deposits in the discharge

zone. This may be due to an insulating effect of the carbon, or it may be due to exothermic recombination reactions occurring at the carbon surface.

With an $\rm H_2/CO$ plasma, the maximum feasible pressure range was found to be 80-100 mm Hg. Above 100 mm, the tube wall in the plasma zone overheated excessively in spite of the cooling air jet. A large fraction of the tube wall heating is due to exothermic recombination reactions that occur at the wall. With an $\rm H_2$ or an $\rm H_2/CO$ plasma, tube wall heating is observed as a dull red glow at pressures above 30 mm Hg; air cooling of the quartz tube is required under these conditions. With an argon plasma, no tube wall heating is observed for plasma pressures as high as 500 mm Hg.

The reason for the difference in tube wall heating effects between H₂ and Ar is that no dissociation reactions occur in an Ar plasma, whereas in a hydrogen plasma, highly endothermic dissociations occur in the plasma zone, and highly exothermic recombinations occur at the tube wall. Bell has indicated that the wall recombination reaction is significant in H₂ plasmas; this observation was confirmed by our experiments, and the results of our kinetic model are also consistant with this.

The $\rm H_2/CO$ plasma has the same blue color as an $\rm H_2$ plasma. However, a very faint greenish-yellow afterglow is observed to extend 5-10 mm downstream of the plasma. This afterglow is probably due to recombination reactions that continue after the gas has left the plasma zone. We may speculate that these reactions only occur downstream of the plasma; however, it is equally likely that they occur to some extent within the plasma, but their emissions are masked by the light emitted by the dominant excitations within the plasma zone.

Several investigators of H_2/CO systems have stressed the importance of quenching. ⁴, ⁵, ⁷ To test this effect, the section of the quartz reactor tube immediately downstream of the plasma zone was packed with dry ice. In our quench experiment, the quench zone was about 3 cm downstream of the plasma zone; this restriction was dictated by the geometry of our microwave cavity. Because of the large diameter of the reactor tube, the contacting of the gases with the chilled walls was not as effective nor as fast as the quench method of Baddour, ⁴, ⁷

who has used a water-cooled probe of very small diameter to withdraw gases directly from the plasma zone. No improvement in conversion was observed in our system, which indicated that our quench arrangement was ineffective. The kinetic model of the reactions in the $\rm H_2/CO$ system explains the importance of rapid quenching, as will be discussed later.

DISCUSSION AND MODELING

A. Reactions of the H₂/CO Plasma System

Table 1 lists the chemical equations used to model the reactions of the discharge zone and of the zone immediately downstream of the discharge. The rate constants listed are those used in the kinetic model. As will be explained later, some of the key rate constants were adjusted to improve the fit of the model to our data.

Some of the rate constants in Table 1 were reported as functions of temperature; to evaluate these, a temperature of 800°K was assumed for the plasma zone and for the region immediately downstream of the plasma. Bell has reported a temperature range of 600°K to 1000°K for a CO/CO₂/O₂ plasma. For those rates that were reported for temperatures outside the range of temperature expected for the plasma, activation energies available for similar reactions were used to estimate the rates at 800°K.

Bell has calculated rate constants for electron-impact dissociations of H_2 and CO. ^{1, 2} These rates are evaluated from reaction cross sections (σ) with the assumption of a Maxwell-Boltzmann distribution of electron energies. Referring to Table 1, the expressions for k_1 and k_2 are given by

$$k = \sqrt{\frac{8}{\pi m_e}} (\kappa T_e)^{-3/2} \int_0^\infty \epsilon \, \sigma(\epsilon) \, \exp(-\epsilon/\kappa T_e) \, d\epsilon$$
 (1)

Bell has successfully used these rate constants to model the dissociation of H₂ and CO in discharges.

Electron impact ionizations also occur, but their influence on the products of the plasma reactions is small. The calculated concentrations of uncharged species (C,H) in the plasma zone are in the range of 10^{15} - 10^{17} atoms/cm³. Charged species must exist at approximately the same concentration as electrons to maintain charge neutrality in the plasma. The electron density of our system was about 10^{12} electrons/cm³. Ionic species would therefore not exceed concentrations of 10^{12} ions/cm³; they would arise from reactions of the general type

$$e + H_2 \rightarrow H_2^+ + 2e$$

 $e + CO \rightarrow CO^+ + 2e$

These ions do react with neutral molecules, but because they are present in concentrations several orders of magnitude smaller than the uncharged atomic species, their contribution to the total product yield was expected to be small. Bell has reached the same conclusion regarding ion reactions in H₂ plasmas.²

The reactions of the plasma system include electron-impact dissociations to C and H (reactions 1 and 2), recombinations to the feed materials (reactions 3, 4, 5), recombinations to hydrocarbons or hydrocarbon intermediates (reactions 6-22), and reactions to CO_2 and H_2O (reactions 23-26). All of the recombinations with the exception of reaction 4 are homogeneous gas-phase reactions. Reaction 4 represents the recombination of H to H_2 at the surface of the tube. The rate expression for the disappearance of H is

$$2R_4 = 2k_4[H] \tag{2}$$

Bell has evaluated the recombination constant from the rate of H atom migration to the tube wall and the recombination coefficent (γ):

$$k_4 = \frac{1}{4} \frac{V_r}{r} \gamma \tag{3}$$

where the random velocity and recombination efficiency are given by

$$V_{r} = \sqrt{\frac{8 \kappa T}{\pi m}}$$
 (4)

$$\gamma = .114 \exp(-1090/T) \tag{5}$$

This heterogeneous recombination is probably a major factor causing the tube wall heating observed in the plasma zone; nearly half the total hydrogen recombination to H₂ occurs via this mechanism.

Although some carbon atoms diffuse to the reactor walls and condense out as an amorphous carbon deposit, the loss by this mechanism is small, as observed in our experiments. No significant heterogeneous recombination of C and O occurs because the condensed carbon is not highly reactive and because O combines rapidly with H or H₂ to form H₂O.

B. Reactor Model

The reaction system was modeled as two isothermal zones: the plasma zone, where dissociations to reactive intermediates occur, and the region downstream of the plasma, where recombinations to hydrocarbon products occur (Figure 9).

1) Plasma Zone (Backmix Reactor)

The reactions occurring in the plasma zone are the electron-impact dissociations of H₂ and CO, and the recombination of H to H₂ and C and O to CO. Recombination reactions of H, C, and O to more complex molecules were assumed not to occur in the plasma zone. Recombination products would be formed in excited states due to the exothermic nature of recombination reactions, and electron impacts in the high energy environment of the discharge would probably cause a large fraction of the recombination products to decompose again.

The assumption that no recombination to hydrocarbons occurs in the plasma zone may not be completely correct; however, this assumption greatly simplifies the mathematical treatment of the zone and adequately predicts the experimental values for the compositions of the end products. The discharge was modeled as a well-mixed (or backmix) reactor. The development of the material balance equations will illustrate the method used.

The material balance is for steady-state generation of the atomic species H, C, and O in the plasma zone; the rate of generation is equal to the rate that the atomic species flow out of the plasma zone:

$$v[H] = V_p(2k_1n_e[H_2] - 2k_3[H]^2 M - 2k_4[H])$$
 (6)

$$v[C] = V_p(k_2 n_e[CO] - k_5[C][O]M)$$
 (7)

The concentration of each species can be written as a function of the conversions of H_2 and CO. For any conversions X_H and X_c , the concentrations of species in the plasma zone are as follows:

$$[H_2] = \frac{M x_{H_2} (1 - X_H)}{x_{H_2} (1 + X_H) + x_{CO} (1 + X_C)}$$
(8)

[H] =
$$\frac{M x_{H_2} (2X_H)}{x_{H_2} (1 + X_H) + x_{CO} (1 + X_C)}$$
 (9)

$$[CO] = \frac{M x_{CO} (1 - X_{C})}{x_{H_{2}} (1 + X_{H}) + x_{CO} (1 + X_{C})}$$
(10)

$$[C] = [O] = \frac{M x_{CO} X_{C}}{x_{H_{2}} (1 + X_{H}) + x_{CO} (1 + X_{C})}$$
(11)

Because the plasma zone is assumed to be well-mixed, the gas flowing out of the zone has the same composition as the gas in the plasma zone. The total volume of gas flowing out of the plasma zone is given by

$$v = v_0 \left[x_{H_2} (1 + X_H) + x_{CO} (1 + X_C) \right]$$
 (12)

Two nonlinear equations in X_H and X_C are obtained by substituting equations 8 - 11 into the material balance equations (6, 7). These equations were solved for X_H and X_C by Newton's method. The conversions were then substituted into equations 8 - 11 to evaluate the concentrations of H, C, O, CO, and H_2 leaving the plasma zone. The residence time in the plasma zone is given by

$$t = V_p/v \tag{13}$$

The electron density (n_e) used in the model was estimated to be about 10^{12} electrons/cm³. It was not possible to measure the electron density directly, but Bell has calculated theoretical estimates of electron density as a function of pressure and absorbed power density for hydrogen discharges. Because the feed used in these experiments was mostly hydrogen, Bell's results were used as an approximation.

The Peclet number, k_1 n_e D_{H-H_2}/U^2 or k_2 n_e D_{C-H_2}/U^2 , is a measure of the amount of axial dispersion in a flow reactor. 35 , 2 For Pe > 1, axial dispersion becomes a significant transport mechanism; axial dispersion results in internal mixing, causing a change from plugflow reactor performance to backmix performance. In the case of the hydrogen reactions considered here, the effect of axial dispersion is significant -- Pe ranges from 0.3 to 370 for the range of flows encountered in our experiment. This indicates that a backmix approximation should apply to the hydrogen dissociation reactions. For the carbon monoxide dissociation reactions, the smaller rate constant and diffusivity result in a Peclet number ranging 4 x 10 -0.6. This would indicate that the carbon reactions should follow a plug

flow model. However, experimental observations to be discussed later indicated that axial dispersion may cause a significant mixing effect for the carbon reactions also. Because of this, and to simplify the calculations and reduce the computation time required for the model, the backmix equations were applied to both the H₂ and the CO reactions. Bell has compared backmix and plug flow models for H₂ dissociation and has found that the backmix approximation best simulates experimental data. ²

A correction for gas bypassing the plasma was also included. This was necessary because of the experimentally observed variations in plasma size, shape, and flow cross section at different pressures and power levels. As mentioned earlier, at pressures above 40 mm Hg, the plasma recedes from the tube walls and becomes asymmetrical. The bypassing factor was based on the ratio of the observed plasma cross sectional area to the reactor flow area.

2) Recombination Zone (Plug Flow Reactor)

After the gases leave the plasma zone, they enter the recombination zone. Reactions 3-26 were applied in this region to calculate the conversion of H, C, and O to stable product molecules. Because the diffusivities of the radicals and molecules formed during the recombination reactions are substantially lower than the diffusivities of H and C atoms, a plug flow model was applied to the recombination zone.

The plug flow model consisted of rate equations for the formation and consumption of each of the species appearing in the reaction scheme; these equations were solved numerically, using the concentrations of H, C, O, H₂, and CO exiting the plasma zone (obtained from Equations 6 and 7) as the initial conditions for the plug flow zone. The following steady state plug flow material balance for any species in the recombination zone can be derived from a balance on a differential element of the recombination zone:

$$U \frac{d n_i}{d 1} = R_i \tag{14}$$

or

$$\frac{d n_i}{dt} = R_i \tag{15}$$

A tabulation of the rate expressions used in the model is shown in Table 3. The solution of this system of equations generates concentration profiles for all the chemical species in the recombination zone.

A simplified model was also developed; it included only the reaction paths leading to CH₄ and C₂H₂. The reactions used in this model are listed in Table 2. This model was streamlined as much as possible to minimize the computation time required while still closely matching the results of the complete model. Both models were tested and were shown to give nearly identical results. The execution time of the simplified model was considerably less than that of the complete model. One reason for this was that the short model did not include the reactions leading to H₂O. Because these reactions occur at an extremely high rate, they were not rate controlling; however, they required a very small step size in the numerical integration. When they were removed, the model (which had a floating step size) could run much faster.

The total reactor model thus consists of the backmix plasma zone and the plug flow recombination zone (including either the complete set of recombination reactions shown in Table 1, or the simplified set shown in Table 2). The model of the plasma zone calculates the concentrations of reactive intermediates H, C, and O generated in the discharge. The model of the recombination zone calculates the concentrations of products that result from the recombination of these intermediates.

C. Data Fitting

The simplified model was used to fit the experimental data shown in Figures 3 and 4 in a regression which adjusted some of the key reaction rate constants. A fast but accurate model was required in order to do the regression using a reasonable amount of computational time. The reaction rates that were adjusted during the regression were k_1 , k_2 , k_3 , k_4 , k_5 , k_9 , k_{11} , and k_{20} . The rates k_1 through k_5 were allowed to float because the total conversion to hydrocarbon products depends directly upon the amount of atomic carbon formed in the plasma (compare Figures 3, 4, and 10), and the CH_4/C_2H_2 ratio depends upon the amount of H generated. The CH_4/C_2H_2 ratio also depends upon k_9 , k_{11} , and k_{20} . The regression routine used Marquardt's method; 36 it was set up to select the rate constants that would minimize the squared deviation between observed and calculated conversions to CH_4 and C_2H_2 . Table 4 compares the results of the regression to the estimates of the rate constants from literature sources.

D. Comparison of Model to Experimental Results

The rates determined from the data shown in Figures 3 and 4 were used in the model; numerical results from the model are compared with our experimental data in Figures 3 - 7. An important observation is that the conversion versus residence time curves (Figures 3, 4) asymptotically approach a limiting value; however, the conversions observed are not equilibrium conversions. Equilibrium studies by the authors and others^{4, 7} have indicated that the observed concentrations of C_2H_2 and CH_4 are not possible at equilibrium in a system at the temperature of our discharge. CH_4 will not be found at equilibrium in a system at a temperature high enough to have the observed concentration of C_2H_2 . The results of our experiments represent a kinetic steady state rather than thermodynamic equilibrium.

This result is readily explained by the proposed kinetic model. For a given yield of C atoms leaving the plasma zone, the $\mathrm{CH_4/C_2H_2}$ ratio is largely determined by the recombination kinetics. The region downstream of the plasma zone is clearly not at chemical equilibrium. As soon as the gases leave the plasma, they begin a quench process in which heat is rapidly lost by radiation. The radicals that are present recombine very rapidly to form stable molecules (Figure 11); there is insufficient time for equilibrium to be established at the low temperatue of the system. The result is that the recombination process is irreversible, and the resulting product concentrations do not represent equilibrium. Instead, they represent the relative ratios of competing irreversible reaction paths.

The asymptotic shapes of the curves of CH₄ and C₂H₂ concentration versus residence time, which resemble an approach to equilibrium, are actually due to kinetic phenomena within the plasma zone. In the plasma zone, the reactions of CO dissociation and recombination reach a steady state independent of flow rate for residence times in excess of 0.20 seconds (see Figure 10); this has the appearance of a system at equilibrium. However, for higher flow rates, the steady state is flow-rate (or residence time) dependent.

To illustrate this, consider a simplified version of the CO dissociation-recombination process:

$$CO + e \xrightarrow{k_2} C + O + e$$

$$CO + M \xleftarrow{k_5} C + O + M$$

By a steady-state material balance for the plasma zone:

$$v[C] = V_p(k_1^n_e[CO] - k_5^M[C][O])$$
 (16)

[C] =
$$\frac{V_{p}^{k_{1}} n_{e}^{n} [CO]}{V_{p}^{k_{5}} M[O] + v}$$
(17)

[C] =
$$\frac{k_1 n_e [CO]}{k_5 M [O] + v/V_p} = \frac{k_1 n_e [CO]}{k_5 M [O] + \frac{1}{t}}$$
 (18)

If $v/v_p << k_2 M[O]$ (low flow rate), then the conversion to carbon atoms will be independent of flow rate, and the system will appear to be at equilibrium:

[C]
$$\approx K \frac{[CO]}{[O]}; K = \frac{k_1^n e}{k_5 M}$$
 (19)

However, if v/V_p is significant in comparison to k_5M [O], then the conversion to carbon atoms will be flow rate dependent. This is the case for residence times less than 0.20 seconds (Figure 10).

By this mechanism, a state of balance between the CO dissociation and recombination reactions gives the appearance of a system at equilibrium, when in fact, most of the reactions occurring in the total reaction system are kinetically limited and are not at equilibrium. For this reason, the product composition cannot be predicted by thermodynamic equilibrium.

The kinetic analysis of our model indicates that the conversion of CO to hydrocarbon products is strongly dependent upon the amount of atomic carbon formed in the plasma zone. This is in contrast to earlier speculation ²⁰ that the conversion was controlled by the amount of H formed in the plasma. The relatively low conversions observed in our system indicate that there is not a significant amount of free radical chain propagation via H such as the following:

$$H + CO \rightarrow CH + O$$

 $H + CO \rightarrow OH + C$

If this were a significant reaction path, higher conversions of CO to hydrocarbons would be expected.

Figure 5 illustrates that the model shows the same dependence upon pressure as was experimentally observed. Figures 6 and 7 show the effect of changes in feed $\rm H_2/CO$ ratio. The model predicts the

conversion of CH_4 very well for 6/1 and 4/1 ratios, and shows the correct trend for a 2/1 ratio. The model fails to predict the correct feed ratio effect for C_2H_2 yields. This indicates that the proposed reaction paths to C_2H_2 are possibly incomplete, or the reactor model is somewhat in error.

The model does correctly predict low conversions to C_2H_4 and C_2H_6 , as was experimentally observed and has been reported by others. ^{5, 6} The low yields of C_2H_4 and C_2H_6 occur because the reaction paths to these products require bimolecular collisions between species that do not reach high concentrations in the recombination zone. C and CH are largely depleted before much CH_4 has been formed, hence reactions 12 and 15 produce little C_2H_4 . The reaction paths to CH_4 favorably compete with the paths to C_2H_6 because they require CH_3 - H_2 or CH_3 -H collisions, which are more likely than CH_3 - CH_3 collisions (Figure 11).

The appearance of narrow bands of soot on the reactor both upstream and downstream of the plasma indicate that the backmix approximation does apply to the carbon reactions as well as to the hydrogen reactions. If there is sufficient axial dispersion to allow carbon atoms to diffuse upstream from the plasma zone, then the plasma zone is probably well mixed.

The importance of rapid quench is evident from the rate of depletion of reactive intermediates in the recombination zone (Figure 11). Carbon atoms disappear very rapidly; nearly all the carbon-containing radicals are depleted with 2 milliseconds of recombination time; H atoms persist somewhat longer. This means that the product distribution is determined with the first 2 milliseconds after the gases leave the plasma region. In our system, this corresponds to about 2 cm of flow distance at high flow rate. For a quench system to have any effect at all, the plasma gases must impinge immediately upon the quench section, and the contacting must be intimate. The high rate of recombination explains why our dry ice quench was ineffective; the recombination reactions were essentially complete before the gases reached the quench zone.

CONCLUSIONS

A kinetic model was developed to describe the dissociation and recombination processes occurring in a complex discharge reaction system. The model was based on two reaction zones: an electronimpact dissociation zone, followed by a zone where free radicals recombine to form hydrocarbon products. The model successfully simulates the residence time and pressure effects observed experimentally. It also explains why discharge reactions appear to approach steady state compositions that are not predicted by thermodynamics. Although it contained many simplifications and approximations, the model was based on a fundamental analysis of the flow processes and chemical reactions occurring in the plasma. The success obtained with this model indicates that kinetic modeling provides a valid analysis of plasma processes. With refinement of the model and more extensive experimental data (such as direct electron density and plasma temperature measurements, accurate measurements of trace products, and perhaps measurements of concentrations of recombination intermediates in a fast-flow experiment), it would probably be possible to completely analyze and quantify the processes occurring in the plasma reactor.

NOTATION

```
^{\mathrm{D}}\mathrm{C} -\mathrm{H}_{2}
                  diffusivity of C through H<sub>2</sub>, cm<sup>2</sup>/sec
                = diffusivity of H through H_2, cm<sup>2</sup>/sec
^{\mathrm{D}}_{\mathrm{H}-\mathrm{H}_{2}}
K
                = constant, dimensionless
k,
                = rate constant
1
                = length, cm
                = total gas density, particles/cm<sup>3</sup>
M
                = particle mass, g
m
m<sub>e</sub>
                = electron mass, g
n<sub>e</sub>
                = electron density, e/cm<sup>3</sup>
                = concentration of species i, atoms/cm<sup>3</sup>
n,
                = reactor radius, cm
r
                = rate, atoms/cm<sup>3</sup>sec
\mathtt{R}_{\mathbf{i}}
                = temperature, <sup>O</sup>K
T
                = residence time, sec
t
                = electron temperature, <sup>o</sup>K
T
                = velocity of gas through plasma, cm/sec
U
                = volume of gas flowing out of plasma zone
                = volumetric flow of reactants into plasma, measured at
v
                   plasma temperature and pressure, cm<sup>3</sup>/sec
                = plasma volume, cm<sup>3</sup>
Vr
                = random velocity, cm/sec
\mathbf{x}_{\mathbf{C}}
                = conversion of CO in plasma zone
                = conversion of H<sub>2</sub> in plasma zone
\mathbf{x}_{\mathbf{H}}
                = mole fraction CO in feed
*CO
x<sub>H2</sub>
                = mole fraction H<sub>2</sub> in feed
                = recombination efficiency
γ
                = energy, eV
\epsilon
                = Boltzmann's constant, erg/molecule OK
                = cross section for reaction. cm<sup>2</sup>
σ
```

= space time in plasma zone, sec

T

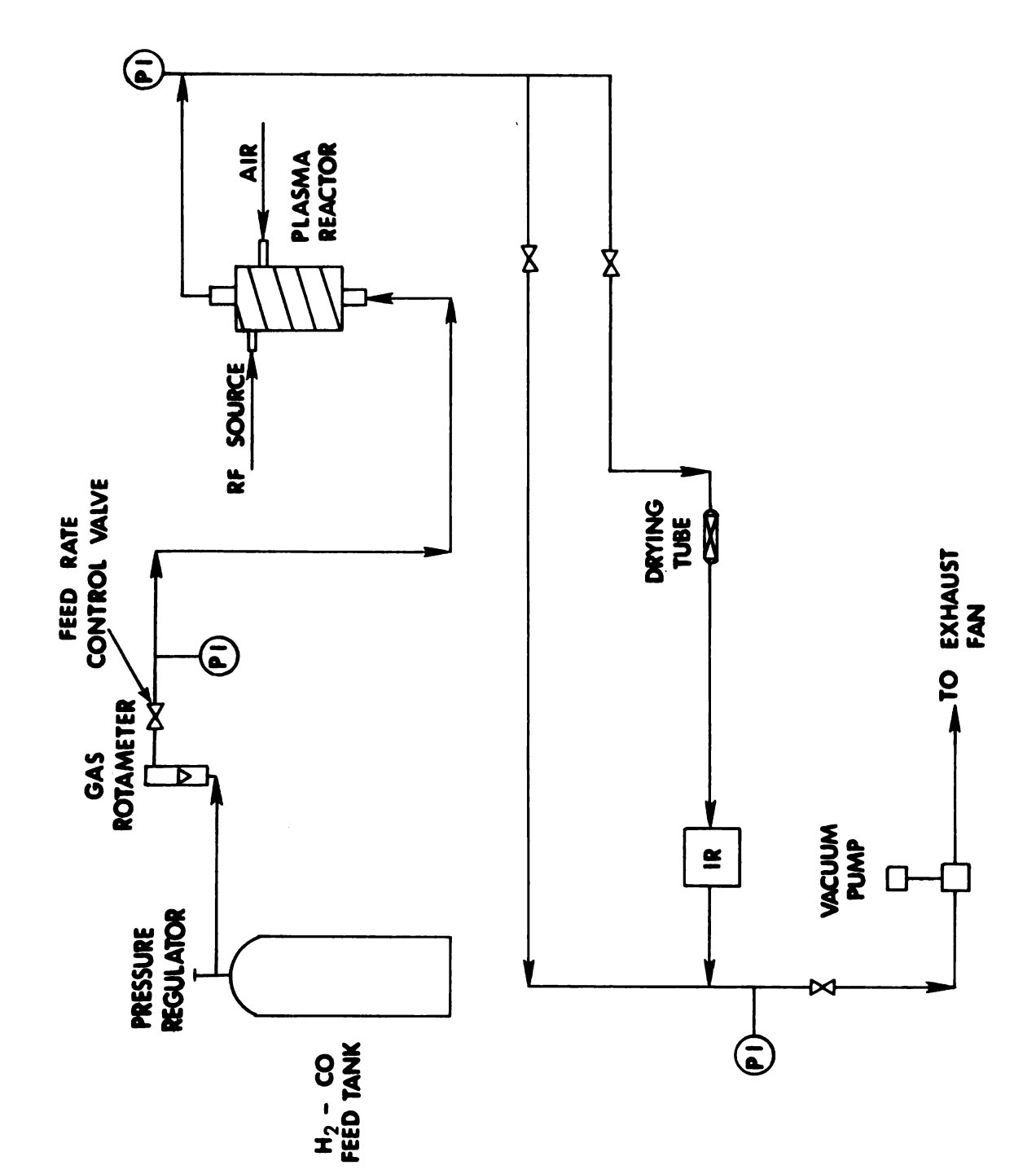


Figure 1 - Plasma reactor flow system

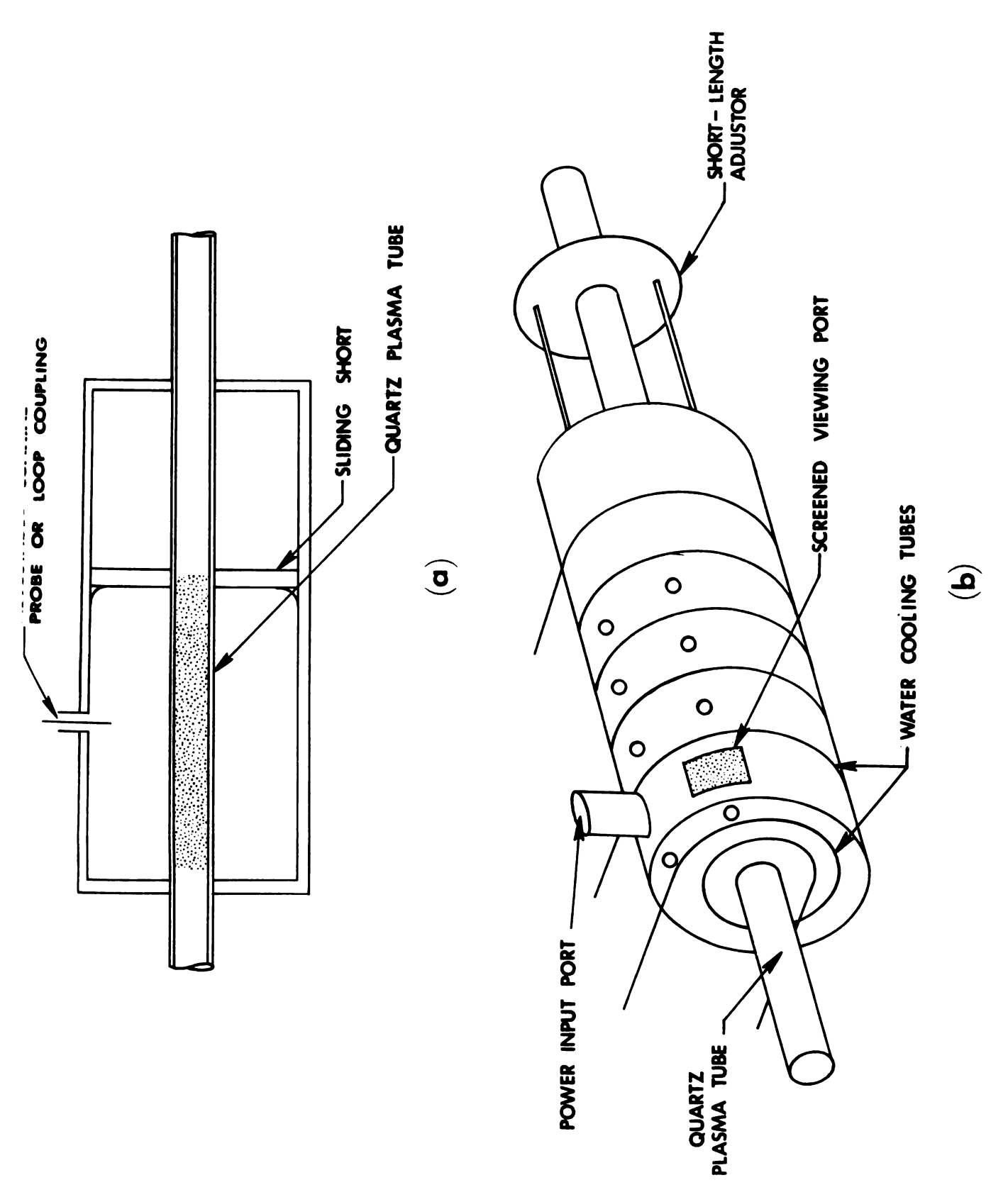
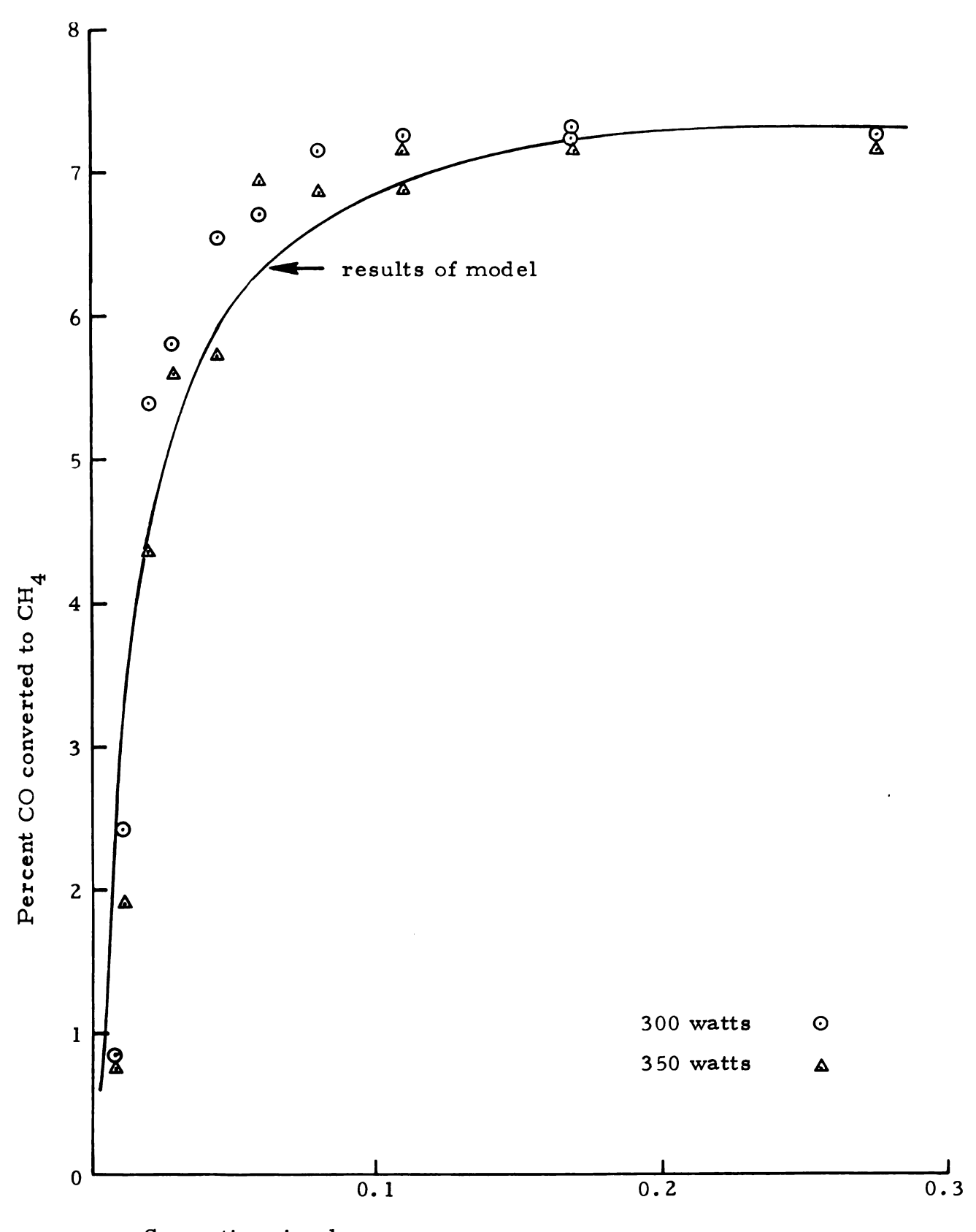


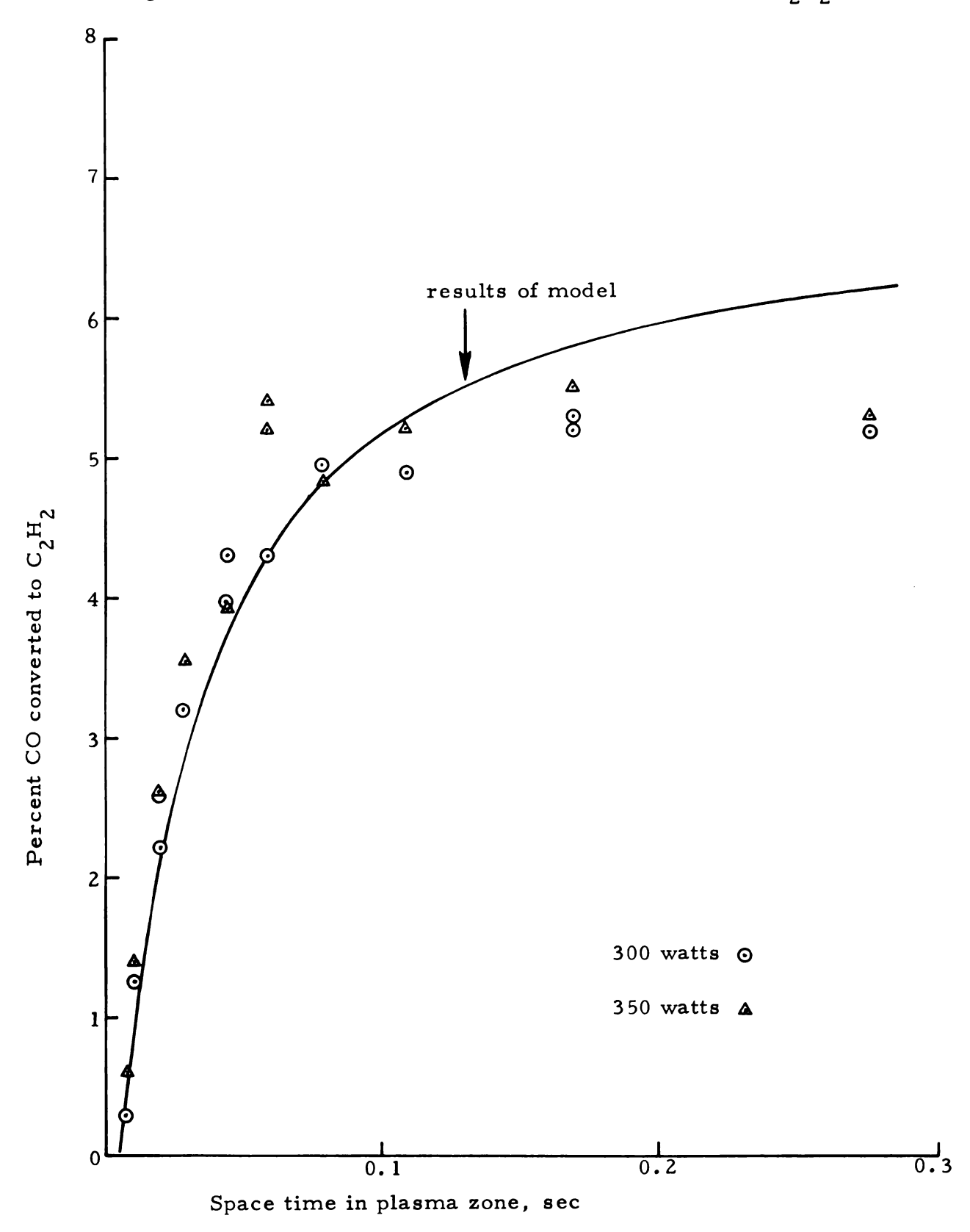
Figure 2- Plasma cavity

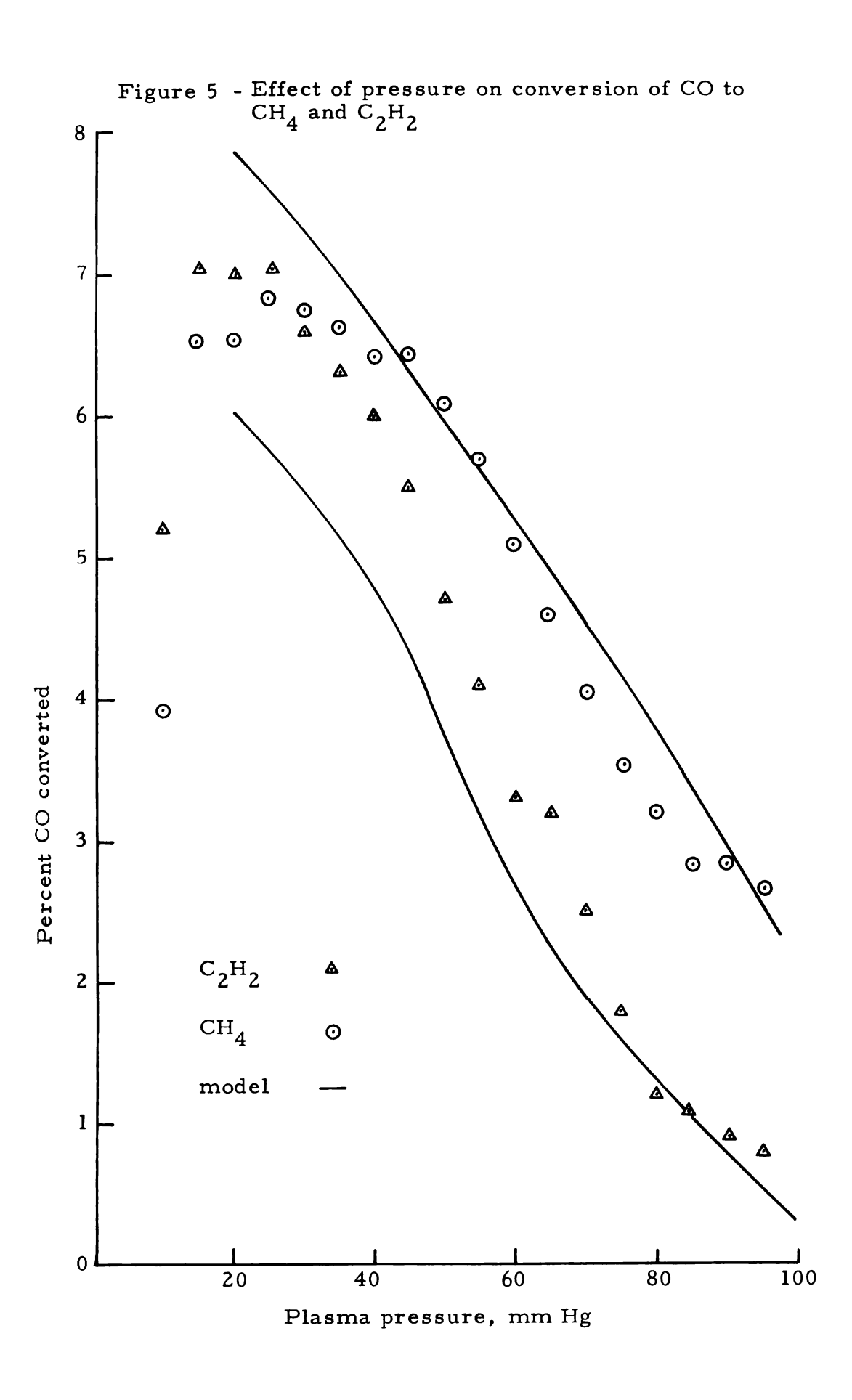
Figure 3 - Effect of space time on conversion of CO to CH₄

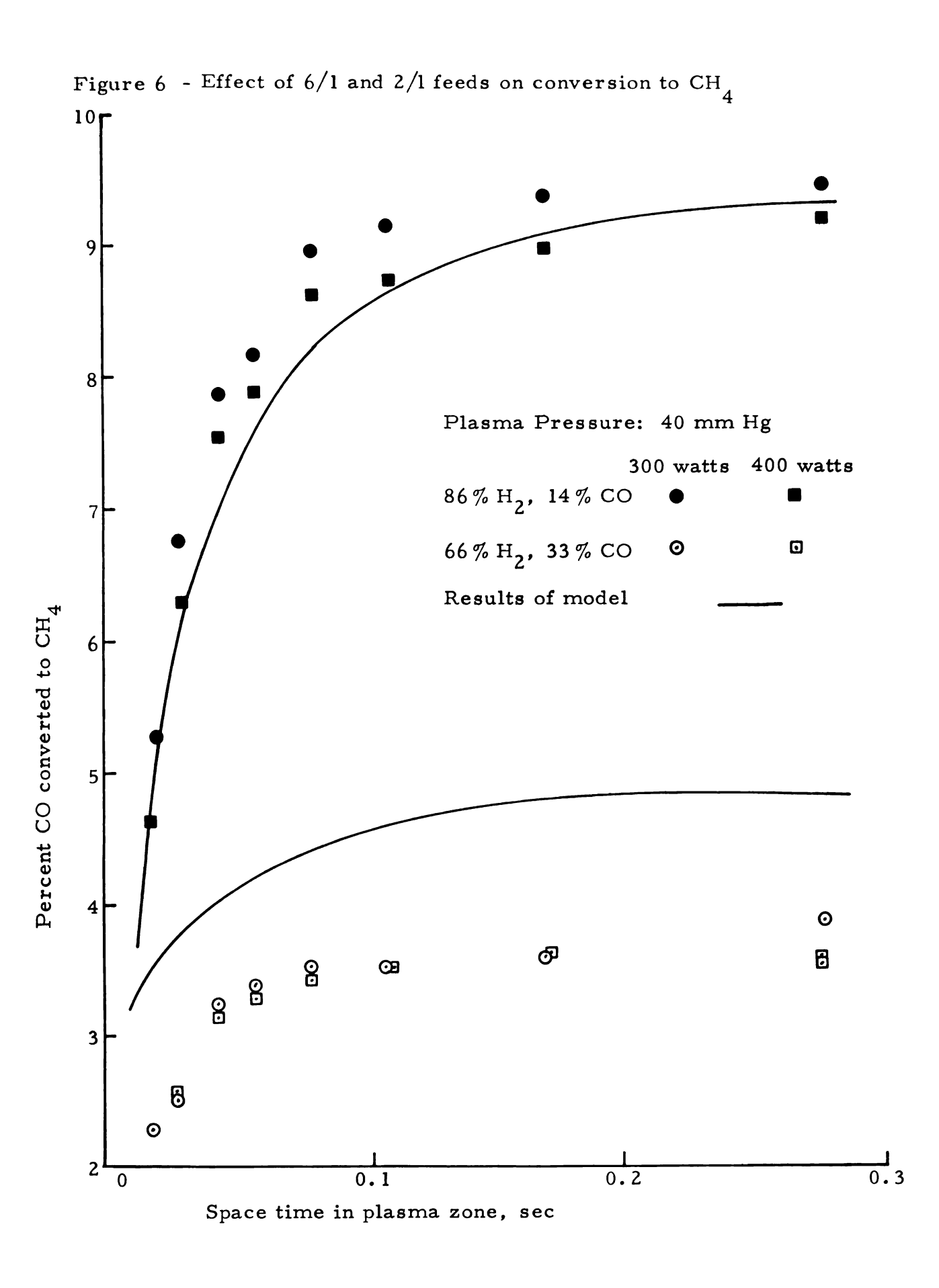


Space time in plasma zone, sec

Figure 4 - Effect of space time on conversion of CO to C_2H_2







Fil

D

Figure 7 - Effect of 6/1 and 2/1 H $_2/CO$ feeds on conversion to C_2H_2

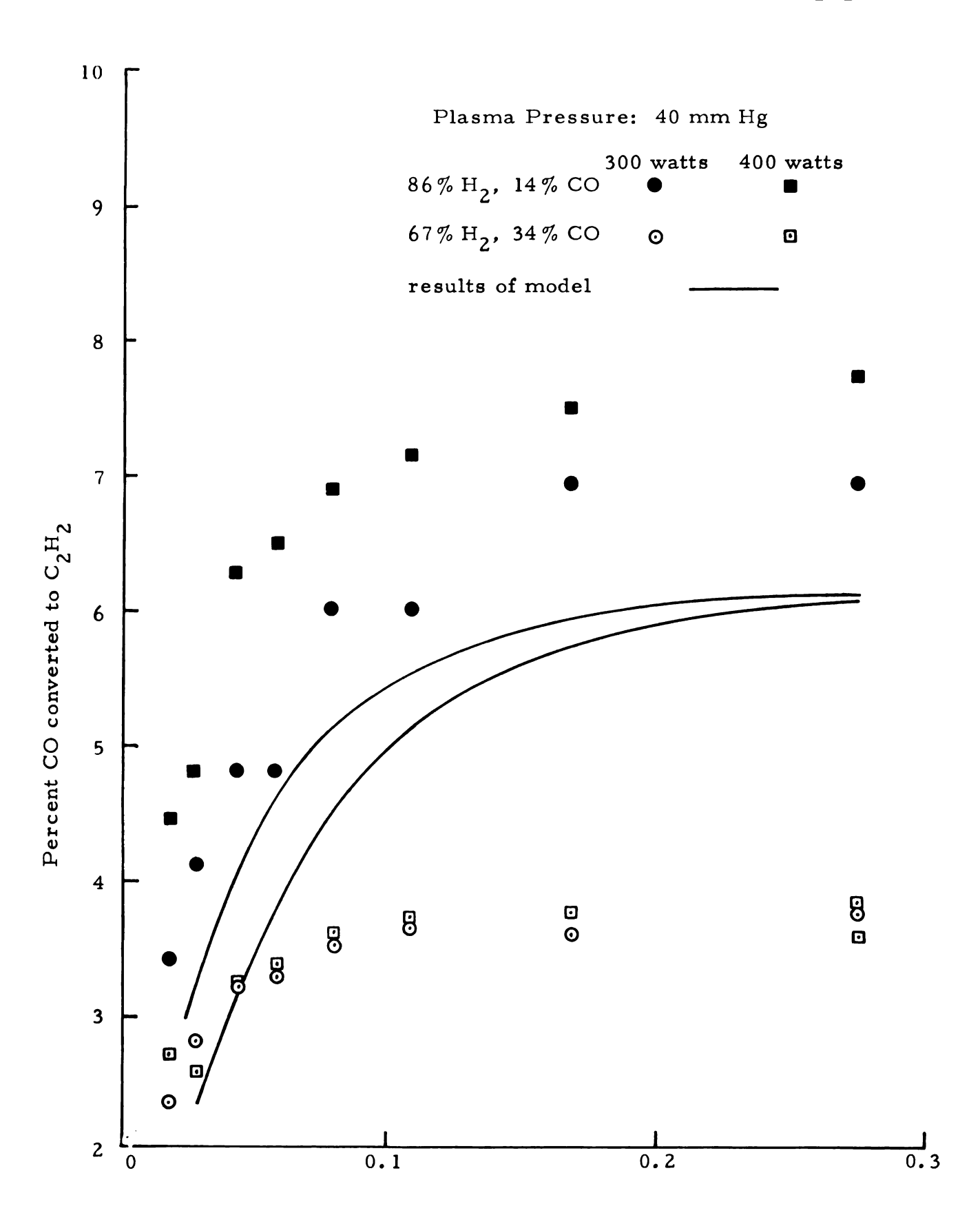
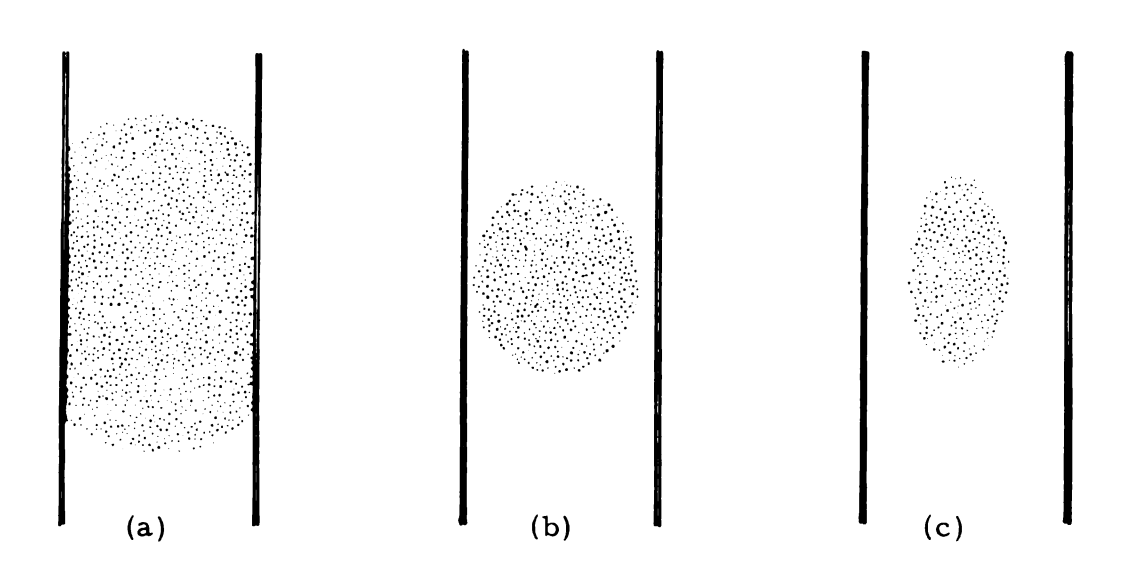


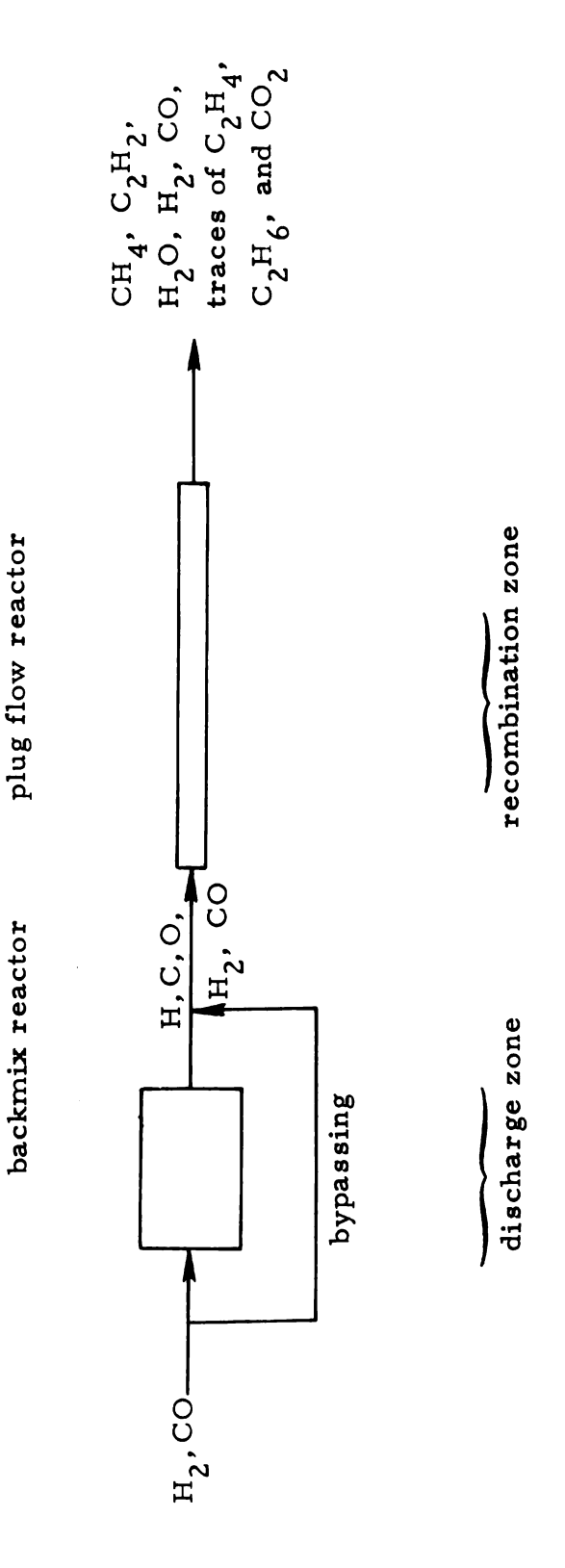
Figure 8 - Effect of pressure on shape of plasma

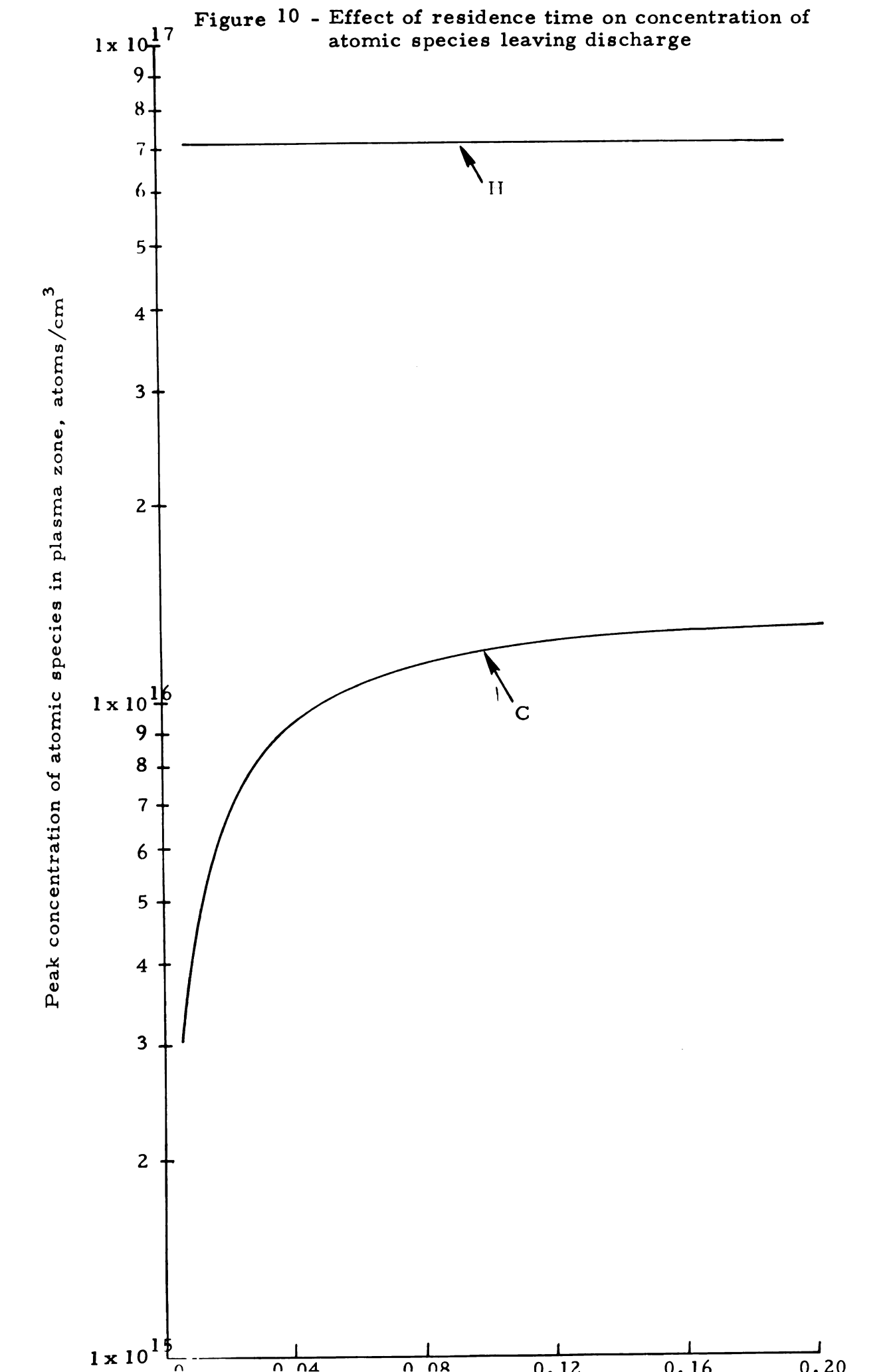


Notes:

- (a) Plasma at pressure of 20 mm Hg
- (b) Plasma at pressure of 40 mm Hg as seen in direction of coaxial microwave probe
- (c) Plasma at pressure of 40 mm Hg as seen at right angles to coaxial microwave probe

Figure 9 - Conceptual model of plasma reactor





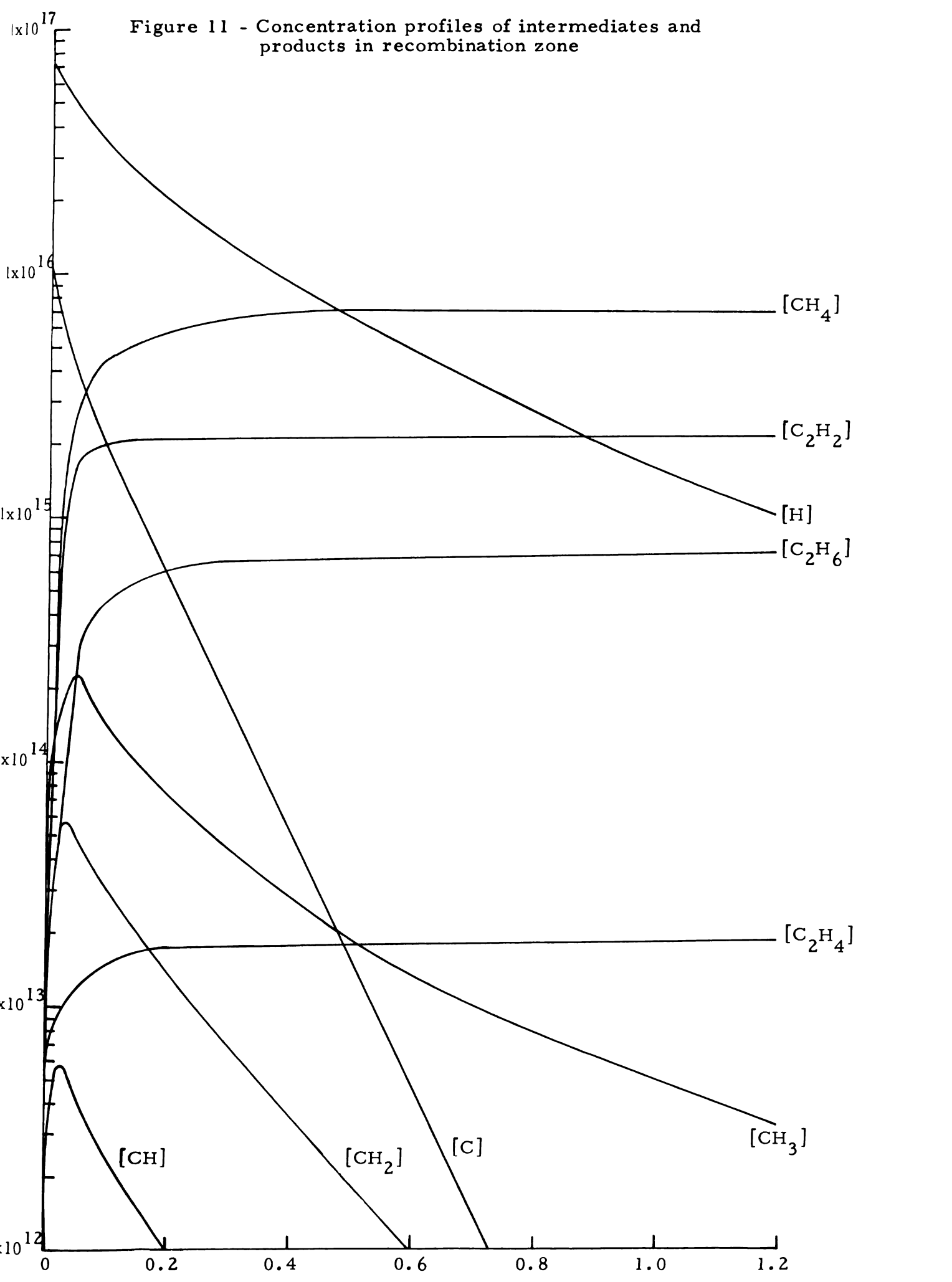


Table 1. Reactions of H_2/CO Plasma System

	Reaction	, k	Reference
1.	$H_2 + e \rightarrow 2H + e$	$2.4 \times 10^{-9} \text{ cm}^3/\text{sec}^*$	(2)
2.	$CO + e \rightarrow C + O + e$	$7.4 \times 10^{-12} \text{ cm}^3/\text{sec}^*$	(1)
3.	$2H + M \rightarrow H_2 + M$	$1.0 \times 10^{-31} \text{ cm}^{6}/\text{sec}^{*}$	(2)
4.	$2H \rightarrow H_2$ (at wall)	$2.5 \times 10^3/\text{sec}^*$	(2)
5.	$C + O + M \rightarrow CO + M$	$2.8 \times 10^{-33} \text{ cm}^{6}/\text{sec}^{*}$	(1)
6.	$C + H_2 \rightarrow CH + H$	$9.5 \times 10^{-17} \text{ cm}^3/\text{sec}$	(27)
7.	$C + OH \rightarrow CH + O$	$8.3 \times 10^{-17} \text{ cm}^3/\text{sec}$	(27)
8.	$C + H + M \rightarrow CH + M$	$2.0 \times 10^{-32} \text{ cm}^6/\text{sec}$	(22)
9.	$2C + M \rightarrow C_2 + M$	$1.2 \times 10^{-30} \text{ cm}^{6}/\text{sec}^{*}$	(22)
10.	$C_2 + H_2 \rightarrow C_2 H_2$	$4.0 \times 10^{-13} \text{ cm}^3/\text{sec}^*$	(est)
11.	$C + H_2 + M \rightarrow CH_2 + M$	$7.0 \times 10^{-32} \text{ cm}^6/\text{sec}$	(20,22)
12.	$C + CH_4 \rightarrow C_2H_4$	$1.0 \times 10^{-15} \text{ cm}^3/\text{sec}$	(20,22)
13.	$CH + H_2 + M \rightarrow CH_3 + M$	$2.1 \times 10^{-30} \text{ cm}^6/\text{sec}$	(25)
14.	$2CH \rightarrow C_2H_2$	$2.0 \times 10^{-10} \text{ cm}^3/\text{sec}$	(22,25)
15.	$CH + CH_4 \rightarrow C_2H_4 + H$	$2.5 \times 10^{-12} \text{ cm}^3/\text{sec}$	(25)
16.	$CH + O \rightarrow OH + C$	$8.8 \times 10^{-12} \text{ cm}^3/\text{sec}$	(27)
17.	$M + CH_2 + H_2 \rightarrow CH_4 + M$	$2.1 \times 10^{-30} \text{ cm}^6/\text{sec}$	(29,30)
18.	$CH_2 + H_2 \rightarrow CH_3 + H$	$1.9 \times 10^{-13} \text{ cm}^3/\text{sec}$	(29)
19.	$CH_2 + CH_2 \rightarrow C_2H_4$	$2.0 \times 10^{-12} \text{ cm}^3/\text{sec}$	(33)
20.	$CH_3 + H + M \rightarrow CH_4 + M$	$3.9 \times 10^{-34} \text{ cm}^6/\text{sec}^*$	(est)
21.	$CH_3 + H_2 \rightarrow CH_4 + H$	$1.2 \times 10^{-15} \text{ cm}^3/\text{sec}$	(21,23,29,30)
22.	$2CH_3 \rightarrow C_2H_6$	$1.2 \times 10^{-10} \text{ cm}^3/\text{sec}$	(24, 26, 29)
23.	$O + H_2 \rightarrow OH + H$	$2.8 \times 10^{-13} \text{ cm}^3/\text{sec}$	(27,31)
24.	$M + OH + H \rightarrow H_2O + M$	$4.0 \times 10^{-25} \text{ cm}^6/\text{sec}$	(31)
25.	$OH + H_2 \rightarrow H_2O + H$	$2.0 \times 10^{-12} \text{ cm}^3/\text{sec}$	(28,31)
26.	$CO + O + M \rightarrow CO_2 + M$	$5.2 \times 10^{-35} \text{ cm}^6/\text{sec}$	(32)

^{*} These rate constants were determined by a regression on the experimental data (see Table 4). All others were estimated from literature sources.

Table 2. Reactions Used in Simplified Model

1.
$$H_2 + e \rightarrow 2H_2$$

2.
$$CO + e \rightarrow C + O + e$$

3.
$$2H + M \rightarrow H_2 + M$$

4.
$$2H \rightarrow H_2$$
 (at wall)

5.
$$C + O + M \rightarrow CO + M$$

6.
$$C + H_2 \rightarrow CH + H$$

8.
$$H + C + M \rightarrow CH + M$$

9.
$$2C + M \rightarrow C_2 + M$$

10.
$$C_2 + H_2 \rightarrow C_2 H_2$$

11.
$$C + H_2 + M \rightarrow CH_2 + M$$

13.
$$CH + H_2 + M \rightarrow CH_3 + M$$

14. 2CH
$$\rightarrow$$
 C₂H₂

17.
$$CH_2 + H_2 + M \rightarrow CH_4 + M$$

18.
$$CH_2 + H_2 \rightarrow CH_3 + H$$

20.
$$CH_3 + H + M \rightarrow CH_4 + M$$

21.
$$CH_3 + H_2 \rightarrow CH_4 + H$$

Table 3. Rate Expressions Used in Recombination Zone.

$$\begin{array}{llll} \frac{dH}{dt} & = & -2k_3[H]^2M - 2k_4[H] + k_6[C][H_2] - k_8[C][H]M + k_{15}[CH][CH_4] \\ & & + k_{18}[CH_2][H_2] - k_{20}[CH_3][H]M + k_{21}[CH_3][H_2] - k_{24}[OH][H]M \\ & & + k_{25}[OH][H_2] \\ \\ \frac{dC}{dt} & = & -k_5[C][O]M - k_6[C][H_2] - k_7[C][OH] - k_8[C][H]M - 2k_9[C]^2M \\ & & - k_{11}[C][H_2]M - k_{12}[C][CH_4] + k_{16}[CH][O] \\ \\ \frac{dO}{dt} & = & -k_5[C][O]M + k_7[C][OH] - k_{16}[CH][O] - k_{23}[O][H_2] - k_{26}[CO][O]M \\ \\ \frac{dC}{dt} & = & k_9[C]^2M - k_{10}[C_2][H_2] \\ \\ \frac{dCH}{dt} & = & k_6[C][H_2] + k_7[C][OH] + k_8[C][H]M - k_{13}[CH][H_2]M - 2k_{14}[CH]^2 \\ & - k_{15}[CH][CH_4] - k_{16}[CH][O] \\ \\ \frac{dCH_2}{dt} & = & k_{11}[C][H_2]M - k_{17}[CH_2][H_2]M - k_{18}[CH_2][H_2] - 2 k_{19}[CH_2]^2 \\ \\ \frac{dCH_3}{dt} & = & k_{13}[CH][H_2]M + k_{18}[CH_2][H_2] - k_{20}[CH_3][H]M - k_{21}[CH_3][H_2] \\ & - 2 k_{22}[CH_3]^2 \\ \\ \frac{dCH_4}{dt} & = & -k_{12}[C][CH_4] - k_{15}[CH][CH_4] + k_{17}[CH_2][H_2]M + k_{20}[CH_3][H]M \\ & + k_{21}[CH_3][H_2] \\ \\ \frac{dC_2H_2}{dt} & = & k_{12}[C][CH_4] + k_{15}[CH][CH_4] + k_{19}[CH_2]^2 \\ \\ \frac{dC_2H_4}{dt} & = & k_{12}[C][CH_4] + k_{15}[CH][CH_4] + k_{19}[CH_2]^2 \\ \\ \frac{dC_2H_4}{dt} & = & k_{22}[CH_3]^2 \\ \\ \frac{dCO}{dt} & = & k_{5}[C][O]M - k_{26}[CO][O]M \\ \\ \frac{dH_2}{dt} & = & k_{3}[H]^2M + k_{4}[H] - k_6[C][H_2] - k_{10}[C_2][H_2] - k_{11}[C][H_2]M \\ & - k_{13}[CH][H_2]M - k_{17}[CH_2][H_2]M - k_{18}[CH_2][H_2] - k_{21}[CH_3][H_2] \\ & - k_{23}[O][H_2] \end{array}$$

$$\frac{dOH}{dt} = -k_7[C][OH] + k_{16}[CH][O] + k_{23}[O][H_2] - k_{24}[OH][H]M - k_{25}[OH][H_2]$$

$$\frac{dH_2O}{dt} = k_{24}[OH][H]M + k_{25}[OH][H_2]$$

$$\frac{dCO_2}{dt} = k_{26}[CO][O]M$$

Table 4. Comparison of Literature Estimates of Rates to Rates from Regression

		k _i	k _i
	Reaction	Literature Estimate	Regression Result
1.	$H_2 + e \rightarrow 2H + e$	1.0×10^{-9}	$2.4 \times 10^{-9} \text{ cm}^3/\text{sec}$
2.	CO + e → C + O + e	7.0×10^{-11}	$7.4 \times 10^{-12} \text{ cm}^3/\text{sec}$
3.	$2H + M \rightarrow H_2 + M$	1.2×10^{-31}	$1.0 \times 10^{-31} \text{ cm}^6/\text{sec}$
4.	$2H \rightarrow H_2$ (at wall)	3.0×10^3	$2.5 \times 10^3 / \text{sec}$
5.	$C + O + M \rightarrow CO + M$	2.9×10^{-33}	$2.8 \times 10^{-33} \text{ cm}^6/\text{sec}$
9.	$2C + M \rightarrow C_2 + M$	1.2×10^{-28}	$1.2 \times 10^{-30} \text{ cm}^6/\text{sec}$
11.	$C + H_2 + M \rightarrow CH_2 + M$	7.1×10^{-32}	$7.0 \times 10^{-32} \text{ cm}^6/\text{sec}$
20.	$CH_3 + H + M \rightarrow CH_4 + M$	-	$3.9 \times 10^{-34} \text{ cm}^6/\text{sec}$

REFERENCES

- 1. Brown, L.C., and A.T. Bell, "Kinetics of the oxidation of carbon monoxide and the decomposition of carbon dioxide in a radio frequency electric discharge," Ind. Eng. Chem. Fundam., 13 (3), 203-218 (1974).
- 2. Bell, A.T., "A model for the dissociation of hydrogen in an electric discharge," Ind. Eng. Chem. Fundam., 11 (2), 209-215 (1972).
- 3. Mearns, A.M., and A.J. Morris, "Oxidation reactions in a microwave discharge: factors affecting efficiency of oxygen atom production," Chem. Eng. Progr. Symposium Series, 67 (112), 37-46 (1971).
- 4. Baddour, R.F., and J.L. Blanchet, "Reactions of carbon vapor with hydrogen and with methane in a high intensity arc," Ind. Eng. Chem. Proc. Des. Develop. 3 (3), 258-266 (1964).
- 5. Blaustein, B.D., and Y.C. Fu, "Hydrocarbons from H₂ + CO and H₂ + CO₂ in microwave discharges: LeChatelier's principle in discharge reactions," Adv. Chem. Ser., <u>80</u>, 259-271, R.F. Gould, ed., Am. Chem. Soc.: Washington D.C. (1969).
- 6. Lett, R.G., W.A. Steiner, and Y.C. Fu, "Mass spectrometry study of microwave discharges in H CO Ar mixtures,"
 J. Phys. Chem., 76 (21), 2941-2946 (1972).
- 7. Baddour, R.F., and J. M. Iwasyk, "Reactions between elemental carbon and hydrogen at temperatures above 2800°K," Ind. Eng. Chem. Proc. Des. Develop. <u>1</u> (3), 169-176 (1962).
- 8. McTaggart, F.K., "Reactions of carbon monoxide in a high-frequency discharge," Aust. J. Chem., 17, 1182-7 (1964).
- 9. Vastola, F.J., P.L. Walker, and J.P. Wightman, "The reaction between carbon and the products of hydrogen, oxygen, and water microwave discharges," Carbon, 1, 11-16 (1963).
- 10. Fu, Y.C., and B.D. Blaustein, "Pyrolysis of coals in a micro-wave discharge," Ind. Eng. Chem. Proc. Des. Develop., 8 (2), 257-262 (1969).
- 11. Fu, Y.C., B.D. Blaustein, and I. Wender, "Gasification of solid fossil fuels in a microwave discharge," Chem. Eng. Prog. Symposium Series, 67 (112), 47-54 (1971).
- 12. Kondratiev, V.N., E.E. Nikitin, and V.L. Talrose, "Problems connected with the investigation of elementary processes in low-temperature plasma," Pure Appl. Chem. 13 (3), 367-387 (1967).
- 13. Polak, L.S., "Chemical Processes in low temperature plasmas," Pure Appl. Chem., 13 (3), 345-360 (1967).

- 14. Bell, A.T., "Models for high frequency electric discharge reactors," Chem. Eng. Prog. Symposium Series, 67 (112), 1-11 (1971).
- 15. Bell, A.T., and K. Kwong, "A model for the kinetics of oxygen dissociation in a microwave discharge," Ind. Eng. Chem. Fundam., 12 (1), 90-94 (1973).
- 16. Bell, A.T., and K. Kwong, "Dissociation of oxygen in a radio-frequency discharge," A.I.Ch.E. Journal, 18 (5), 990-998 (1972).
- 17. Bell, A.T., "Spatial distribution of electron density and electric field strength in a high frequency discharge," Ind. Eng. Chem. Fundam., 9 (1), 160-164 (1970).
- 18. Maksimov, A.I., "Electron density and energy in a microwave helium discharge," Sov. Phys.-Tech. Phys., 11 (10), 1318-1321 (1967).
- 19. Asmussen, J., R. Mallavarpu, J.R. Hamann, and H.C. Park, "The design of a microwave plasma cavity," Proc. I.E.E.E., 62 (1), 109-117 (1974).
- 20. Mertz, S.F., J. Asmussen, and M.C. Hawley, "An experimental study of reactions of CO and H₂ in a continuous flow microwave discharge reactor," IEEE Trans. Plasma Science, <u>PS-2</u> (4), 297-307 (1974).
- 21. Husain, D., and L.J. Kirsch, "Reactions of atomic carbon by kinetic absorption spectroscopy in the vacuum ultra-violet," Trans. Faraday Soc., 67 (7), 2025-2035 (1971).
- 22. Shapiro, J.S., and R.E. Weston, Jr., "Kinetic isotope effects in the reaction of methyl radicals with molecular hydrogen,"
 J. Phys. Chem., 76 (12), 1669-1679 (1972).
- 23. Martinotti, F.F., M.J. Welch, A.P. Wolf, "The reactivity of thermal carbon atoms in the gas phase," Chem. Comm. (J. Chem. Soc. D), (3), 115-116 (1968).
- 24. Walker, R.W., "Activation energies of the reversible reaction between hydrogen atoms and methane to give hydrogen and methyl radicals," J. Chem. Soc. (A), 2391-2398 (1968).
- 25. Basco, N., D.G.L. James, and R.D. Suart, "A quantitative study of alkyl radical reactions by kinetic spectroscopy: Part I," Int. J. Chem. Kin., 2, 215-234 (1970).
- 26. Brown, W., J.R. McNesby, A.M. Bass, "Flash photolysis of methane in the vacuum ultraviolet. II: absolute rate constants for reactions of CH with methane, hydrogen, and nitrogen," J. Chem. Phys., 46 (6), 2071-2080 (1967).

- 27. Umanski, U.M., and A.D. Stepukhovich, "The recombination of radicals at low pressures," Russ. J. Phys. Chem., 43 (8), 1148-1151 (1969).
- 28. Mayer, S.W., and L. Schieler, "Computed activation energies and rate constants for forward and reverse transfers of hydrogen atoms," J. Phys. Chem., 72 (1), 236-240 (1968).
- 29. Dean, A.M., and G.B. Kistiokowsky, "Oxidation of carbon monoxide/methane mixtures in shock waves," J. Chem. Phys., 54 (4), 1718-1725 (1971).
- 30. Bell, J.A., and G.B. Kistiakowsky, "The reactions methylene. VI: the addition of methylene to hydrogen and methane,"
 J. Am. Chem. Soc., 84 (18), 3417-3425 (1962).
- 31. Powell-Wiffen, J. W., and R.P. Wayne, "The reactions of methylene with hydrogens," Photochem. Photobiol., 8, 131-140 (1968).
- 32. Bahn, G.S., Reaction Rate Compilation for the H-O-N System, Gordon and Breach, Science Publishers, 74-99 (1968).
- 33. Brabbs, T.A., and F.E. Belles, "Recombination of carbon monoxide and atomic oxygen at high temperatures," Symp. (Int.) Combus., 11, 125-135 (1967).
- 34. Lee, P.S.T., R.L. Russel, and F.S. Rowland, "The reactions of triplet methylene with alkyl radicals in ordinary photolysis systems," Chem. Comm. (J. Chem. Soc. D), (3), 18-19 (1970).
- 35. Petersen, E.E., Chemical Reactions Analysis, Prentice-Hall, Englewood Cliffs, N. J., p. 199 (1965).
- 36. Kuester, J.L., and J.H. Mize, Optimization Techniques with Fortran, McGraw-Hill, New York, pp. 240-250 (1973).

APPENDIX

Fortran Listing of
Regression Program and
Simplified Reactor Model

```
PROGRAM FIT (INFUT, OUTPUT)
C---THIS PROGRAM DOES A MULTIVARIABLE NON-LINEAR REGRESSION.
C---THE PROGRAM PARAMETERS ARE AS FOLLOWS . . .
     NN=NUMBER OF DATA POINTS
     KK=NUMBER OF UNKNOWNS TO BE FOUND
C
     B=VECTOP OF UNKNOWNS
C
     BMIN=VECTOR OF MINIMUM VALUES OF B
C
C
     BMAX=VECTOR OF MAXIMUM VALUES OF B
C
     X=VECTOP OF INDEPENDENT VARIABLE DATA POINTS
     Y=VECTOR OF DEPENDENT VARIABLE DATA POINTS
С
     PHELEAST SQUAPES OBJECTIVE FUNCTION
C
     Z=COMPUTED VALUES OF THE INDEPENDENT VARIABLE
C
C
     BV=CONTROL PARAMETER--SET TO 1 FOR NUMERICAL DERIVATIVES.
       SET TO -1 FOR ANALYTICAL DERIVATIVES
C
C---THE REGPESSION EQUATION IS OF THE FORM
              Y=F(X,B)
C---THE MATH PROGRAM AND THE SUBROUTINES SHOULD BE DIMENSIONED AS
C---FOLLOWS . . .
     DIMENSION P(NN *K\zeta), A(\zeta K, KK+2), AC(KK, KK+2), X(NN), B(KK), Z(NN),
     Y(NN), BV(KK), 3MIN(KK), 3MAX(KK), FV(KK), DV(KK)
C
C---THE INPUT VARIABLES ARE AS FOLLOWS . . .
C
       X(1,I)=INLET MOLE FRACTION Ha
C
       X(2.1)=INLET MOLE FRACTION CO
C
       X(3,I)=ROTAMETER VOLUMETRIC FLOW, CM3/SEC AT 5PSIG, 300 DEG K
       X(4,I)=PLASMA VOLUME, CM3
Ç
       X(5,I)=FRACTION OF GAS PASSING THRU PLASMA
C
C
       x(6.I)=ELECTRON DENSITY X 10-12, ELECTRONS/CM3
C
       X(7,I)=PLASMA PRESSURE, ATM
C
       X(8,I)=PLASMA TEMPERATURE, DEG K
       YORS(1,1) = PERCENT CONVERSION CO TO CH4
C
       YOUS(2, I) = PERCENT CONVERSION CO TO C2H2
      DIMENSION P(70), A(7,9), AC(7,9), B(7), Z(10), Y(10), BV(7), BMIN(7),
          BMAX (7), FV (7), DV (7), YO3S (2, 10), K (16), X(8, 10)
      EXTERNAL FUNC
      COMMON X
      COMMON/BFUNC/YOBS, PRFLAG, K, M
      REAL K.M
      ICNT=0
C---READ NUMBER OF DATA POINTS (NN), NUMBER OF UNKNOWNS (KK), AND
C---PRINT PARAMETER (PRELAGI-- +1 GIVES DIAGNOSTIC PRINTOUT, -1 SUPPRESSES
      READ 801, NN, KK, PRFLAG
  801 FORMAT (2I10,F10.0)
C--- READ INITIAL GUESSES OF UNKNOWNS (B)
      READ 805, (B(J), J=1, K<)
  805 FORMAT (8E10.4)
C---READ LIMITS ON VARIABLES
      READ 805, (3MIN(J), J=1, K()
      READ 805, (BMAX(J), J=1, K<)
      PRINT 808
  808 FORMAT (*1*,4x,*+2*,9x,*>0*,8x,*?VF*,9X,*PV*,8X,*FTP*,9X,*NE*,9X,
          *PP*,9X,*PT*,9X,*CH4*,8X,*C2H2*)
C---READ INDEPENDENT AND DEPENDENT VARIABLES. EACH CARD CORRESPONDS
```

```
C---TO A DATA POINT AND GIVES INFORMATION ON PLASMA CONDITIONS AND YIELD
      DO 97 I=1.NN
      READ 805, (X(J, I), J=1, B), (YOBS(J, I), J=1, 2)
  805 FOPMAT (10E8.0)
C---CONVERT ELECTRON FROM INPUT UNITS TO ACTUAL UNITS OF E/CM3
   97 X(6, I) = X(6, I) + 1 \cdot E12
C---READ IN KNOWN VALUES OF RATE CONSTANTS
      READ 806 \cdot (K(I) \cdot I = 1.15)
      DO 98 T=1.NN
      PRINT 809, (X(J,I), J=1,8), YOBS(1,I), YOBS(2,I)
  809 FORMAT(1X,10(G10.3,1X))
   98 Y(I)=0.
      PRINT 810
  810 FORMAT (*0*)
      FNU=0.
      FLA=0.
      TAU=D.
      EFS=0.
      PHMIN= 0.
      I = 0
      KD=KK
      DO 100 J=1.KK
      FV(J)=0
      BV(J)=1
  100 CONTINUE
      ICON=KK
C---ICON IS THE NUMBER OF JNCONVERGED UNKNOWNS
      ITER = 0
  200 CALL BSOLVE(KK,B,NN,Z,Y,PH,FNU,FLA,TAU,EPS,PHMIN,I,ICON,FV,
          DV, 3V, 3MIN, 3MAX, P, FUNC, DERIV, KD, A, AC, GAMM)
     1
      ITER=ITER+1
      PRINT 807, ITER, ICON, PH
  807 FORMAT(* AFTER*,I4,* ITERATIONS,*,I4,* UNKNOWNS ARE NOT CONVERGED.
     1 THE VALUE OF THE DBJECTIVE FUNCTION IS*, E15.8)
C---CHECK TO SEE IF ALL UNKNOWNS ARE CONVERGED
      PRFSAV=PPFLAG
      IF(ITER/2*2 .NE. ITER) GO TO 202
      PRFLAG=1.
      CALL FUNC (KK, B, NN, Z, FV)
      PRFLAG=PRFSAV
  202 CONTINUE
      IF(ICON) 10,300,200
   10 IF (ICON+1) 20,50,200
   20 IF(ICON+2) 33,73,200
   30 IF(ICON+3) 40,80,200
   40 IF(ICON+4) 50,90,209
   50 GO TO 95
   60 PRINT 820
  820 FORMAT(//* NO FUNCTION IMPROVEMENT POSSIBLE*)
      GO TO 300
   70 PPINT 821
 821 FORMAT(//, * THERE ARE MORE UNKNOWNS THAN FUNCTIONS*)
      GO TO 300
   80 PRINT 822
 822 FORMAT(//* TOTAL VARIABLES ARE ZERO*)
```

```
GO TO 300
 90 PRINT 823
 823 FORMAT(//,2x, *CORRECTIONS SATISFY CONVERGENCE REQUIREMENTS, BUT LA
    1MDA FACTOR (FLA) STI_L _ARGE.*)
     GO TO 300
 95 PRINT 824
 824 FORMAT(//, * THIS IS NOT POSSIBLE*)
     GO TO 300
 300 PRINT A25
 825 FORMAT(//, * THE SOLUTIONS OF THE EQUATIONS ARE AS FOLLOWS . . .*)
     00 400 J=1,KK
     PRINT 826, J.B(J)
 826 FORMAT(/,2X,*B(*,T2,*) = *,E15.8)
400 CONTINUE
     PRFLAG=1.0
    CALL FUNC (KK, B, NN, 7, FV)
1000 CONTINUE
     END
```

```
FUNCTION ARCOS(Z)

X=Z

KFY=0

IF(X.LT.(-1.)) X=-1.

IF(X.GT.1.) X=1.

IF(X.GF.(-1.) .ANJ. X.LT.0.0)KEY = 1

IF(X.LT.0.0) X=ABS(X)

IF(X.E0.0.0) GO TO 10

ARCOS=ATAN(SQRT(1.-X*X)/X)

IF(KFY.EQ.1) ARCOS=3.14159265-APCOS

GO TO 999

10 APCOS=1.5707963

999 RETUPN

FND
```

```
SUBROUTINE BSOLVE(KK, B, NN, Z, Y, PH, FNU, FLA, TAU, EPS, PHMIN, I, ICON, FV,
           DV.BV. BMIN. BMAX, P. FUNC, DERIV, KD. A. AC. GAMM)
       DIMENSION P(70), A(7, 3), AC(7, 3), B(7), Z(10), Y(10), BV(7), BMIN(7),
           BMAX(7), FV(7), DV(7), YOBS(2, 10), X(8, 10)
       N = NN
       K=KK
       KP1=K+1
       KP2=K+2
       KBI1=K*N
       KBT2=KBI1+K
       KZI=KBT2+K
       IF(FNU.LE.D.) FNU=10.
       IF(FLA.LE.D.) F.A=0.01
       IF (TAU.LE.O.) TAU=0.J01
       IF(FPS.LE. 0.) EPS=0.00002
       IF (PHMIN.LE.O.) PHMIN=O.
   120 KE=0
   130 DO 160 T1=1.K
   160 IF (BV(I1).NE.O.) KE=KE+1
       IF(KE.GT.0) GO TO 170
   162 ICON=-3
  163 GO TO 2120
  170 IF(N.GE.KE) GO TO 500
  180 ICON=-2
  190 GO TO 2120
  500 I1=1
  530 IF(I.GT.0) GO TO 1530
  550 DO 560 J1=1.K
       J2=KBI1+J1
       P(J2) = B(J1)
       J3=KBI2+J1
  560 P(J3) = ABS(B(J1)) + .01
       GO TO 1031
  590 IF(PHMIN.GT.PH.AND.I.GT.1) GO TO 625
       DO 620 J1=1.K
       N1 = (J1 - 1) + N
       TF(BV(J1)) 601,520,605
  601 CALL DERIV(K, B, N, Z, P(N1+1), FV, DV, J1, JTEST)
       IF(JTEST.NE.(-1)) GO TO 620
       BV(J1)=1.
  605 DO 606 J2=1,K
       J3=KBI1+J2
  606 P(J3) = P(J2)
       J3=KBI1+J1
       J4=KBI2+J1
C---INCREMENT VARIABLES TO TEST SLOPE OF OBJECTIVE FUNCTION
       DEN=0.01*AMAX1(P(J4),ARS(P(J3)))
       IF(P(J3)+DEN .LE. 344X(J1)) GO TO 55
       P(J3) = P(J3) - NEN
       DEN=-DFN
       GO TO 56
   55 P(J3)=P(J3)+0EN
   56 CALL FUNC(K,P(K9I1+1),N,P(N1+1),FV)
       DO 610 J2=1,N
```

```
JB=J2+N1
  610 P(JB) = (P(J3) - Z(J2)) / DEN
  620 CONTINUE
C---SET UP CORRECTION FQUATIONS
  625 DO 725 J1=1,K
      N1 = (J1 - 1) * N
      A(J1.KP1) = 0.
      IF(BV(J1))630,632,631
  630 00 640 J2=1.N
      N2 = N1 + J2
  640 A(J1,KP1) = A(J1,(P1)+2(N2)*(Y(J2)-Z(J2))
  650 DO 680 J2=1.K
  660 A(J1,J2)=0.
  565 N2=(J2-1)*N
  670 DO 680 J3=1.N
  672 N3=N1+J3
  674 N4=N2+J3
  680 A(J1,J2) = A(J1,J2) + P(N3) + P(N4)
      IF(A(J1,J1).GT.1.0E-20) GO TO 725
  692 DO 694 J2=1,KP1
  694 A(J1,J2)=0.
  695 A(J1,J1)=1.0
  725 CONTINUE
      GN = 0
      00 729 J1=1.K
  729 GN=GN+A(J1,KP1)**2
C---SCALE COPRECTION FACTORS
      DO 726 J1=1,K
  726 A(J1,KP2)=SQRT(A(J1,J1))
      DO 727 J1=1,K
      A(J1,KP1) = A(J1,KP1)/A(J1,KP2)
      DO 727 J2=1,K
  727 A(J1,J2)=A(J1,J2)/(A(J1,KP2)*A(J2,KP2))
  730 FL=FLA/FNU
      GO TO RIN
  800 FL=FNU*FL
  810 DO 840 J1=1,K
  820 DO 830 J2=1,KP1
  830 AC(J1,J2) = \Lambda(J1,J2)
  840 AC(J1,J1) = AC(J1,J1) + = L
C---SOLVE THE CORRECTION EQUATIONS
      DO 930 L1=1,K
      L2=L1+1
      DO 910 L3=L2,KP1
  910 AC(L1,L3) = AC(L1,L3)/AC(L1,L1)
      00 930 L3=1,K
      TF(L1-L3) 920,930,920
  920 DO 925 L4=L2, KP1
  925 AC(L3,L4) = AC(L3,L4) - AC(L1,L4)*AC(L3,L1)
  930 CONTINUE
      DN = 0.
      DG = 0.
      DO 1028 J1=1.K
      AC(J1,KP2)=AC(J1,KP1)/A(J1,KP2)
      J2=KBI1+J1
```

```
P(J2) = AMAX1 (3MIN(J1), AMIN1(BMAX(J1), B(J1) +AC(J1, KP2)))
      DG=DG+AC(J1,KP2) *A(J1,KP1) *A(J1,KP2)
      DN=DN+AC(J1,KP2)+AC(J1,KP2)
 1028 AC(J1, KP2) = P(J2) - B(J1)
      COSG=DG/SQRT(DN*GN)
      JGAM=0
      IF(COSG) 1100,1110,1110
 1100 JGAM=2
      COSG = - COSG
 1110 CONTINUE
      COSG=AMIN1 (COSG, 1.0)
      GAMM=APCOS(COSG) *180./3.14159265
      IF (JGAM.GT.D) GAMM=180.-GAMM
 1030 CALL FUNC(K,P(K9I1+1),N,P(KZI+1),FV)
 1500 PHT=0.
      DO 1520 JI=1,N
      J2=KZI+J1
 1520 PHI=PHT+(P(J2)-Y(J1))**2
      IF(PHI.LT.1.0E-10) GO TO 3000
      IF(I.GT.0) GO TO 1540
 1521 ICON=K
      GO TO 2110
 1540 IF(PHI.GE.PH) GO TO 1530
C---EPSILON TEST FOR JONVERGENCE
 1200 ICON=0
      NO 1220 J1=1,K
      J2=KBI1+J1
 1220 IF(ABS(AC(J1,KP2))/(TAU+ABS(P(J2))).GT.EPS) ICON=ICON+1
      IF(ICON.EQ.U) 30 TO 1400
C---GAMMA LAMDA TEST
      IF (FL.GT.1.0 .AND. GAMM.GT.90.0) ICON=-1
      GO TO 2105
C---GAMMA EPSTLON TEST
1400 IF(FL.GT.1.0 .AND. GAMM.LE.45) ICON=-4
      GO TO 2105
1530 IF(I1-2) 1531,1531,2310
1531 I1=I1+1
      GO TO (530,590,8J0),I1
2310 IF(FL.LT.1.0E8) GO TO 800
1320 ICON=-1
2105 FLA=FL
      DO 2091 J2=1,K
     J3=KBI1+J2
2091 B(J2) = P(J3)
2110 DO 2050 J2=1,N
     J3=KZT+J2
2050 Z(J2) = P(J3)
     PH=PHI
     I = I + 1
2120 RETURN
3000 ICON=0
     GO TO 2105
     END
```

799 FORMAT(//, * K1=*,10(E11.4,1X),/, * K11=*,6(E11.4,1X))

IF(PRFLAG.LT.0.0) GO TO 26 PRINT 799,(K(I),I=1,16)

C---GAS DENSITY, MOLECULES/CM3

26 CONTINUE DTPR=.001

```
C---CONVERT FLOW RATE FROM ROTAMETER CONDITIONS TO PLASMA CONDITIONS
      VFR=Y(3.J) +67.33
C---CALCULATE COMPOSITION LEAVING PLASMA ZONE
      CALL PLASMA(X(7,J),VFR,X(4,J),X(1,J),X(2,J),X(8,J),X(5,J),
          H2,C0,H,C,0,T,X(5,J)
      TOTCARB=CO+C
       TPR=T+NTPR
      TMAX=T+16.*DTPR
      CH=0.$CH2=0.8CH3=0.8CH4=0.8C2=0.8C2H2=0.
       IF(PPFLAG.LT. 0) GO TO 25
      PRINT 800
  800 FORMAT(//,6X, +T+,11X, +H2+,10X, +CO+,10X, +H+,11X, +C+,11X, +C2+,10X,
           *CH*,10X, *CH2*,9X, *CH3*,9X, *CH4*,8X, *C2H2*)
     1
      PRINT 801.T.H2.C0.H,S.C2.CH.CH2.CH3.CH4.C2H2
  801 FORMAT(/,11(1X,E11.4))
   25 CONTINUE
C---ADJUST C ATOM CONSENTRATION TO REFLECT THE FRACTION CONVERTED
    TO CO2. C2H4. AND C2H5.
      C=0.905*C
C---NO ADJUSTMENT OF THE HIGONCENTRATION MAY BE REQUIRED BECAUSE THE
    REACTIONS OMITTED TO SIMPLIFY GENERATE AS WELL AS CONSUME H
      DCODT=0.
C---CALCULATE REAUTIONS DOWNSTREAM OF PLASMA BY EULERS METHOD
   20 CONTINUE
      DT = .0001
C FOR C+H2=CH+H
      R3=K(3)*C*H2
C FOR C+C+M=C2+M
      R4=K(4)*C*C*M
C FOR C2+H2=C2H2
      R5=K(5)*C2*H2
C FOR C+H2+M=GH2+M
      R6=K(6)*C*H2*M
C FOR CH+H2+M=CH3+M
      R7=K(7)*CH*H2*M
C FOR 2 CH=C2H2
      R8=K(8)*CH*CH
C FOR CH2+H2+M=GH4+M
      R9=K(9)*CH2*H2*4
C FOR CH2+H2=CH3+H
      P10=K(10) *CH2*H2
C FOR CH3+H+M=CH4+M
      R11=K(11) *CH3*H*Y
C FOR CH3+H2=CH4+H
      R12=K(12) *CH3*H2
C FOR H+C+M=CH+M
      R13=K(13)*H*C*M
C FOR 2H+M=H2+M
      R14=K(14)*H*H*M
C FOR 2H=H2 AT THE WALL
      R15=K(15)*H
      DH2DT=-R3-R5-R6-X7-R9-R10-R12+R14+R15
      DCH4DT=R9+R11+R12
      DC2H2DT=R5+R8
      DHDT=R3+R10-R11+R12-R13-2.*(R14+R15)
```

```
DCDT=-F3-R4-74-R5-P13
      DCHDT=R3-R7-R8-R8+P13
      OCH2DT=R6-R9-R10
      DCH3DT=R7+R10-R11-R12
      DC2DT=R4-R3
  110 CONTINUE
      DO 120 T=2,4
      CN(I) = A(I) + D(I) + DT
  120 CONTINUE
C----CHECK TO SEF THAT NO SPECIES CONCENTRATIONS ARE BEING DRIVEN
                USF SMALLER STEP SIZE IF NECESSARY.
     NEGATIVE.
      DO 122 I=5.10
      CN(I) = A(I) + D(I) + DT
      IF(CN(I).GE.0.0) GO TO 122
      DT=0.75*A(I)/(A(I)-CN(I))*DT
      GO TO 110
  122 CONTINUE
      T = I + DT
      DO 130I=2.10
      A(I) = CN(I)
  130 CONTINUE
      IF(T.GE.TMAX) SO TO 30
      IF(T.LT.TPR) GO TO 20
      TPR=TPR+NTPP
      IF(PRFLAG.LT.D) GO TO 125
      PRINT 801, T, H2, 30, H, 3, C2, CH, CH2, CH3, CH4, C2H2
  125 CONTINUE
C----EXIT LOOP WHEN REACTIVE INTERMEDIATES ARE SUFFICIENTLY DEPLETED.
      IF(AMAX1(H.C.C2.CH.3H2.3H3)/AMIN1(CH4.C2H2) .LT. 0.01) GO TO 31
      GO TO 20
   30 CONTINUE
      IF(PRFLAG.LT.O) GO TO 31
      PRINT 801, T, H2, 30, H, 3, C2, CH, CH2, CH3, CH4, C2H2
   31 CONTINUE
C--- GALCULATE CONVERSIONS TO CH4 AND C2H2
      CCH4=CH4/TOTCAR3*100.
      CC2H2=2. *C2H2/TOTCARB*100.
C---CHECK TO SEE THAT ALL REACTIVE INTERMEDIATES ARE BEING CONSUMED
      CONSTR1=1.
       BASE COMPARISON ON ACTUAL OBSERVED CONCENTRATIONS . . .
C - - -
      CH4A=YOUS(1,J)*FOTCARB/100.
      C2H2A=Y03S(2,J)*FOTC4RB/100.
      IF (AMAX1 (H, C, CH, CH2, C2)/AMIN1 (CH4A, C2H2A) .LE. 0.01) GO TO 35
      CONSTP1=5.
      PRINT 802
  802 FORMAT(* -----CONSTRAINT APPLIED FOR HIGH RESIDUAL CONCENTRATION O
     1F REACTIVE INTERMEDIATES -----*)
   35 CONTINUE
C---MOST CH3 REMAINING WOULD NORMALLY GO TO C2H6, SO CHECK THAT
                                                                     THE
    CH3 LEVEL IS NOT EXCESSIVE . . .
      CONSTR2=1.
      IF (CH3/CH4A .LE. 0.1) GO TO 35
      CONSTR2=5.0
      PRINT 804
  804 FORMAT(* ----CONSTRAINT APPLIED FOR HTGH CH3 CONCENTRATION----*)
```

C

```
36 CONTINUE
Z(J)=ABS(CCH4-YOBS(1,J))+ARS(CC2H2-YOBS(2,J))
IF(PRFLAG.LT.O.) GO TO 27
PRINT 803,J,CCH4,YOBS(1,J),CC2H2,YOBS(2,J),T,Z(J)
803 FORMAT(* DATA CARD*,I3,* CH4 (CALC,ORS),*,2(1X,G10.3),* C2H2 (CALC 1,OBS),*,2(1X,G10.3),* T=*,G10.3,* Z=*,G10.3)
27 CONTINUE
RETURN
END
```

```
SUBROUTINE PLASMA(P.VFR.PV.XH2I.XCOI.PT.NE.H2.CO.H.C.O.TIME.FTP)
 C---THIS SUBPOUTINF CALCULATES THE DISSOCIATION PRODUCTS FORMED IN
                 THE PLASMA ZONE IS ASSUMED TO BE WELL MIXED AND
 C---THE PLASMA.
 C---NO RECOMPINATIONS ARE ASSUMED TO OCCUR OTHER THAN THOSE OF H2 AND CO.
 C---P=PRESSUPE, ATM
 C---VFR=VOLUMETRIC FLOW RATE, CM3/SEC
 C---PV=PLASMA VOLUME, CM3
 C---XH2I, XCOI=INLFT MOLE FRACTIONS H2 AND CO
 C---PT=PLASMA TEMPERATURE, DEG K
 C---NE=ELECTRON DENSITY, F/CM3
 C --- K1 FOR H2 + E = 2+ + E (C43/SEC)
 C---K2 FOR 2H+M=H2+M, CM5/SEC
 C---KW FOR 2 H =H2 AT WALL (/SEC)
 C=-K4 FOR CO + E = C + O + F (CM3/SEC)
 C --- K5 FOR C + O + M = CO + M (CM6/SFC)
      COMMON/BEUNC/YOBS (2,10), PRELAG, K (16), M
      REAL K, K1, K2, KW, K4, K5, M, NE
      XH2=XH2I $ XCO=XCOI
C---SET VALUES OF RATE CONSTANTS
      K1=K(1)
      K2=K(14)
      KW=K(15)
      K4 = K(2)
       K5=K(15)
C---CONCENTRATION OF H2 AND CD (MOLECULES/CM3)
C---SOLVE BACKMIX MATERIAL BALANCES FOR H2 AND CO DISSOCIATION BY
    SIMULTANFOUS APPLICATION OF NEWTONS METHOD TO H AND C MTL BALANCES
      XH=0.1 $ XC=0.1
      IT=0
C----CALCULATE CONVERSION LEAVING THE PLASMA ZONE
   20 CONTINUE
      IT=IT+1
      ALPHA=XH2*(1.+XH)+XC)*(1.+XC)
      FH=PV/VFR+(K1*NE*(1.-XH)/ALPHA-K2+M+M+XH2+4.*XH+XH/(ALPHA+ALPHA)
           -KW+2. *XH/ALPHA) -XH
      FHP=-PV/VFR*((K1*NF+2.*<W)/ALPHA+8.*K2*M*M*XH2*XH/(ALPHA+ALPHA))-
     1
           1.
      XH=XH-FH/FHP
       \Delta LPHA = XH2 + (1. + XH) + XCO + (1. + XC)
      FC=PV/VFR*(K4*NE*(1.-XC)/ALPH4-K5*M*M*XCO*XC*XC/(ALPH4*ALPH4))-XC
      FCP=-PV/VFR*(K4*NE/ALPH4+2.*K5*M*M*XCO*XC/(ALPHA*ALPHA))-1.
       XC=XC-FC/FCP
       TF(IT.6T.10) GO TO 22
      IF(ABS(FC).GT.0.001 .OR. ABS(FH).GT.0.001) GO TO 20
      GO TO 23
   22 PRINT 701
  701 FORMAT(*---- NEWIONS METHOD NOT CONVERGED-----*)
   23 CONTINUE
C----CONVERT CONVERSIONS TO CONCENTRATIONS
      H2=M*XH2*(1.-XH)/ALPH4
      H=M*XH2*2.*XH/ALPHA
      CO=M*XCO*(1.-XC)/ALPHA
```

```
C=M*XCO*XC/ALPHA

0=C
TIMF=PV/(VFP*ALPHA)

C ADJUST OUTLET GAS CONSENTRATIONS TO ACCOUNT FOR GAS BYPASSING

C FTP IS THE FRACTION OF GAS THAT PASSES THROUGH PLASMA ZONE

H=FTP*H

C=FTP*C

0=FTP*D

H2=(1.-FTP) *M*X42I+FTP*+2

CO=(1.-FTP) *M*X30I+FTP*30

RETURN
END
```

œ

			+ 3 3 1 1 1 1 1 1 1 1 1 1 1 1 1 1 1 1 1	5.2E+00	+ 111 -+ •	• 3±+	0.55+00	+1:5.	. 9E+	+ .+ -	1.95-13	
		0.	~	.2E+	• 4E+	.9E+0	0.75+33	.75+B	.3E+0	.9E+0	<mark>-</mark>	
1		100	• 0E+0	• 9E+	• 0E+0	. JE+1	8.05+02	• 0E+0	• 0E+1	• 0E+3	E-1	
1.	.001	0 0	·26E-	.26E-	.26E-	.26E-	5.26E-2	.26E-	.26E-	.26E-	.1E-3	
1.	.001	10001	• 0E+	. JE+9	.0E+J	. OF + U	1.0E+J0	• 0E+0	.05+3	• 0E+0	.1E-3	.0
•	001	10 10.	3E+	int Til	5E+	5E+	.755+00	5E+	5 F F F	75E+	0 E-	0
+		00.	1.03E+1	1.035+1	0	035+		035	035+	Û3E	0.0	0.
+	.001	100	8E+	4114	3≡+	₹ 0	1.935+1	9 11 4	111	315	55-	96
+	.0091	1300.	0.2E+00	0.2E+00	<u>+</u>	•2E+	t.	.5	2E+	•2	0.0	1.2F-15
•	001	1000.	.8E+00	+	+ W	+	.8E+30	+	+ ω	+ u:	0.	05-32

Fortran Listing of
Complete Reactor Model

```
PROGRAM TEST(INPUT, OUTPUT)
     DIMENSION B (7), Z(10)
     COMMON/BFUNC/YOBS(2,10), PRFLAG, K(30), M
     COMMON X (8, 10)
     PEAL K, M
     READ 801, NN, KK, PRFLAG
 801 FORMAT(2110,F10.0)
C---NN IS NUMBER OF DATA CARDS, KK IS NUMBER OF FLOATING PARAMETERS
     FEAD 805, (B(J), J=1, KK)
 805 FORMAT (8E10.4)
      CO 10 I=1.NN
     PEAD 806, (X(J,I),J=1,8), (YOBS(J,I),J=1,2)
 806 FORMAT (1CE8.2)
     X(6,I)=X(6,I)+1.0E12
  10 CONTINUE
     PEAD 806, (K(I), I=1,30)
     CALL FUNC (KK, B, NN, Z, FV)
     END
```

```
SUBROUTINE PLASMA(P, VFR, PV, XH2I, XCOI, PT, NE, H2, CO, H, C, O, TIME, FTP)
 C---THIS SUBROUTINE CALCULATES THE DISSOCIATION PRODUCTS FORMED IN
 C---THE PLASMA. THE PLASMA ZONE IS ASSUMED TO BE WELL MIXED AND
 C---NO RECOMBINATIONS ARE ASSUMED TO OCCUR OTHER THAN THOSE OF H2 AND CO.
 C---P=PRESSURE, ATM
 C---VFR=VOLUMETRIC FLOW RATE, CM3/SEC
 C---PV=PLASMA VOLUME, CM3
 C---XH2I, XCOI=INLET MOLE FRACTIONS H2 AND CO
 C---PT=PLASMA TEMPERATURE, DEG K
 C---NE=ELECTRON DENSITY, E/CM3
 C -- - K1 FOR H2 + E = 2H + E (CM3/SEC)
 C---K2 FOR 2H+M=H2+M, CM6/SEC
 C---KW FOR 2 H = H2 AT WALL (/SEC)
 C --- K4 FOR CO + E = C + O + E (CM3/SEC)
 C --- K5 FOR C + O + M = CO + M (CM6/SEC)
       COMMON/BFUNC/YOBS(2,10), PRFLAG, K(30), M
       PEAL K, K1, K2, KW, K4, K5, M, NE
       XH2=XH2I $ XCO=XCOI
C---SET VALUES OF RATE CONSTANTS
       K1 = K(1)
       K2 = K(28)
       KW = K(29)
       K4=K(9)
       K5 = K(30)
C---SOLVE BACKMIX MATERIAL BALANCES FOR H2 AND CO DISSOCIATION BY
     SIMULTANEOUS APPLICATION OF NEWTONS METHOD TO H AND C MTL BALANCES
       XH=0.1 $ XC=0.1
       IT=D
C----CALCULATE CONVERSION LEAVING THE PLASMA ZONE
      XH IS CONVERSION OF H2 TO H, XC IS CONVERSION OF CO TO C
   20 CONTINUE
       IT=IT+1
       ALPHA = XH2 + (1.+XH) + XCO + (1.+XC)
       FH=PV/VFR+(K1+NE+(1.-XH)/ALPHA-K2+M+M+XH2+4.+XH+XH/(ALPHA+ALPHA)
           -KW+2. +XH/ALPHA) -XH
       FHP=-PV/VFR+((K1+NE+2.+KW)/ALPHA+8.+K2+M+M+XH2+XH/(ALPHA+ALPHA))-
           1.
       XH=XH-FH/FHP
       ALPHA = XH2*(1.+XH) + XCO*(1.+XC)
       FC=PV/VFR*(K4*NE*(1.-XC)/ALPHA-K5*M*M*XCO*XC*XC/(ALPHA*ALPHA))-XC
       FCP=-PV/VFR+(K4+NE/ALPHA+2.+K5+M+M+XCO+XC/(ALPHA+ALPHA))-1.
       XC=XC-FC/FCP
       IF(IT.GT.10) GO TO 22
       IF (ABS(FC).GT.0.001 .OR. ABS(FH).GT.0.001) GO TO 20
       GO TO 23
   22 FRINT 701
  701 FORMAT(*---- NEWTONS METHOD NOT CONVERGED-----*)
   23 CONTINUE
C----CONVERT CONVERSIONS TO CONCENTRATIONS
       H2=M+XH2+(1.-XH)/ALPHA
       H=MFXH2F2.FXH/ALPHA
       CO=M+XCO+(1.-XC)/ALPHA
```

```
C=M*XCO*XC/ALPHA

O=C

TIME=FV/(VFR*ALPHA)

C ADJUST OUTLET GAS CONCENTRATIONS TO ACCOUNT FOR GAS BYPASSING

C FTP IS THE FRACTION OF GAS THAT PASSES THROUGH PLASMA ZONE

H=FTP*H

C=FTP*C

O=FTP*O

H2=(1.-FTP)*M*XH2I+FTP*H2

CO=(1.-FTP)*M*XCOI+FTP*CO

FETURN
ENO
```

```
SUBROUTINE FUNC(KK, B, NN, Z, FV)
C
C---THIS ROUTINE CALCULATES THE CONVERSION OF CO AND H2 TO VARIOUS
C---PRODUCTS BY RECOMBINATION OF H, C, AND O DCWNSTREAM OF THE PLASMA
C
      EQUIVALENCE (A(1), H2), (A(2), CO), (A(3), H), (A(4), C), (A(5), O),
     1
           (A(6),CH),(A(7),CH2),(A(8),CH3),(A(9),CH4),(A(10),C2H2),
     2
           (A(11),C2H4),(A(12),C2H6),(A(13),OH),(A(14),C2),(A(15),CO2),
     3
           (A(16), H20), (D(1), DH2DT), (D(2), DC ODT), (D(3), DHDT), (D(4), DCDT),
           (D(5), DODT), (D(6), DCHOT), (D(7), DCH2DT), (D(8), DCH3DT),
           (0(9),0CH4DT),(0(10),0C2H2DT),(0(11),0C2H4DT),(0(12),0C2H6DT),
     5
           (D(13), DOHDT), (D(14), DC2DT), (D(15), DC02DT), (D(16), DH20DT)
      DIMENSION A (16), D(16), CN(16)
      COMMON/BFUNC/YOBS, PRFLAG, K, M
      COMMON X (8.10)
      DIMENSION Z(10), B(7), YOBS(2,10), K(30)
      REAL K, NE, M
C
       X(1, I) = INLET MOLE FRACTION H2
       X(2,I)=INLET MOLE FRACTION CO
C
C
       X(3,1)=ROTAMETER VOLUMETRIC FLOW, CM3/SEC AT 5PSIG, 300 DEG K
C
       X(4,I)=PLASMA VOLUME, CM3
C
       X(5,1)=FRACTION OF GAS PASSING THRU PLASMA
C
        X(6, I) = ELECTRON DENSITY X 10-12, ELECTRONS/CM3
C
       X(7,I)=PLASMA PRESSURE, ATM
C
       X(8,I)=PLASMA TEMPERATURE, DEG K
C
       YOBS (1, I) = PERCENT CONVERSION CO TO CH4
C
       YOBS(2, I) = PERCENT CONVERSION CO TO C2H2
C
      IF (PRFLAG.LT.J.O) GO TO 26
      PRINT 799, (K(I), I=1, 30)
  799 FORMAT(//,* K1 =*,10(G10.3,2X),/,* K11=*,1J(G10.3,2X),/,
           * K21=*,10(G10,3,2X))
   26 CONTINUE
      OTPR=.0005
C---AS THE ROUTINE CYCLES THRU THE LOOP, IT EVALUATES THE EXIT
C---COMPOSITION AT EACH OF NN DATA POINTS
      DO 27 J=1, NN
C---M=GAS MOLECULES/CM3=P*(NAVOGADRO/R)/T
      M=X(7,J)*7.345E21/X(8,J)
C---CONVERT FLOW RATE FROM ROTAMETER CONDITIONS TO PLASMA CONDITIONS
       VFR=X(3,J)*X(8,J)/300.*1.34/X(7,J)
C---CALCULATE COMPOSITION LEAVING PLASMA ZONE
      CALL PLASMA(X(7,J),VFR,X(4,J),X(1,J),X(2,J),X(8,J),X(6,J),
     1
           H2,C0,H,C,0,T,X(5,J)
      TPR=T+DTPR
      CH=0.$CH2=0.$CH3=0.$CH4=0.$C2H2=0.$C2H4=0.$C2H6=0.$OH=0.$C2=0.
      CO2=0. $H20=0.
      TMAX=T+16.*DTPR
      IF (PRFLAG.LT. 0) GO TO 25
      PRINT 800
      PRINT 801, T, H2, C0, H, C, O, CH, CH2, CH3, CH4, C2H2, C2H4, C2H6, OH, C2, CO2,
     1
           H20
   25 CONTINUE
```

C---CALCULATE REACTIONS DOWNSTREAM OF PLASMA BY EULERS METHOD

```
20 CONTINUE
      DT = . 0001
C FOR M+CO+0=CO2+M
      R2=K(2)*C0*0*M
C FOR C+H2=CH+H
      R3=K(3)*C*H2
C FOR C+OH=CH+O
      F4=K(4) + C+OH
 FOR C+C+M=C2+M
      P5=K(5) + C+C+M
C FOR C2+H2=C2H2
      R6=K(6) *C2*H2
C FOR C+H2+M=CH2+M
      R7=K(7) + C+H2+M
C FOR C+CH4=C2H4
      R8=K(8)*C*CH4
C FOR CH+H2+M=CH3+M
      P13=K(10)*CH *H2*M
 FOR CH+CH=C2H2
      P11=K(11)*CH*CH
C FOR CH+CH4=C2H4+H
      F12=K(12)*CH*CH4
 FOR CH+0=OH+C
      P13=K(13)*CH*O
 FOR CH2+H2+M=CH4+M
      R14=K(14) *CH2*H2*M
 FOR CH2+H2=CH3+H
      R15=K(15)+CH2+H2
 FOR CH2+CH2=C2H4
      P16=K(16) + CH2+CH2
 FOR CH3+H+M=CH4+M
      P18=K(18) + CH3+H+M
C FOR CH3+H2=CH4+H
      R19=K(19)*CH3*H2
 FOR CH3+CH3=C2H6
      F20=K(20) +CH3+CH3
C FOR 0+H2=OH+H
      F21=K(21) +0+H2
C FOR M+ 0H+ H= H20+ M
      R22=K (22) + M + OH + H
C FOR 0H+H2=H20+H
      F23=K(23)+OH+H2
C FOR H+C+M=CH+M
      P24=K(24)*H*C*M
C FOR H+CO=CH+O
      P25=K(25)*H*C0
C FOR H+CO=C+OH
      P26=K(26)*H*C0
C FOR H2+2H=2H2
      P27=K(27) + H2+H+H
C FOR 2H+M=H2+M
      R28=K(28)*H*H*M
C FOR 2H=H2 AT THE TUBE WALL
      P29=K(29)*H
```

G FOR C+O+M=CO+M

, -

```
F3C=K(30)*C*O*M
      DH2DT=-R3-R6-R7-R10-R14-R15-R19-R21-R23+R27+R28+R29-R18
      DCODT=-R25-R26-R2+R30
      DHDT=R3+R12+R15+R19+R21-R22+R23-R24-R25-R26-2.*R27-2.*R28-R29
      DCDT=-R4-2. *R5-R7-R3+R13-R24+R26-R30
      DODT=R4-R13-R21+R25-R30-R2
      DCHDT=R3+R4-R10-2. *R11-R12-R13+R24+R25
      DCH2DT=R7-R14-R15-2.*R16
      DCH3DT=R10+R15-R19-2.*R20-R18
      DCH4DT=-P8-R12+R14+R18+R19
      DC2H2DT=R6+R11
      DC2H4DT=R8+R12+R16
      DC 2H6DT=R20
      D0HDT=-R4+R13+R21-R22-R23+R26
      DC 20T=R5-R6
      DCO2DT=R2
      DH20DT=R23+R22
  110 CONTINUE
      DO 120 I=1,16
      CN(I) = A(I) + D(I) + DT
      IF(CN(I).GE.O.O) GO TO 120
      DT=0.75*A(I)/(A(I)-CN(I))*DT
      GO TO 110
  120 CONTINUE
      T=T+DT
      DO 130 I=1,16
      A(I) = CN(I)
  130 CONTINUE
      IF (T.GE.TMAX) GO TO 30
      IF (T.LT. TPR) GO TO 20
      TPR=TPR+DTPR
      IF(PRFLAG.LT.0) GO TO 125
      PRINT 801, T, H2, C0, H, C, O, CH, CH2, CH3, CH4, C2H2, C2H4, G2H6, OH, G2, CO2,
          H20
  800 FORMAT(//,7x,+T+,9x,+H2/CH4+,4x,+CO/C2H2+,7x,+H/C2H4+,6x,+C/C2H6+,
          6x, *0/0H*, 8x, *CH/C2*, 5x, *CH2/C02*, 5x, *CH3/H2O*)
  801 FORMAT(/,9(E12.4),/,12X,8E12.4)
  125 CONTINUE
      IF(AMAX1(H,C,O,CH,CH2,CH3,OH,C2)/AMIN1(CH4,C2H2).LT. 0.01)GO TO 31
      GO TO 20
   30 CONTINUE
      IF (PRFLAG.LT.0) GO TO 31
      PRINT 801,T,H2,C0,H,C,O,CH,CH2,CH3,CH4,C2H2,C2H4,C2H6,OH,C2,CO2,
          H20
   31 CONTINUE
C---CALCULATE CONVERSIONS TO CH4 AND C2H2
      TOTCARB=C0+C+CH+CH2+CH3+CH4+C02+2.*(C2H2+C2H4+C2H6+C2)
      CCH4=CH4/TOTCARB *100.
      CC2H2=2. *C2H2/TOTCARB*100.
C---CHECK TO SEE THAT ALL REACTIVE INTERMEDIATES ARE BEING CONSUMED
      CONSTR1=1.
       BASE COMPARISON ON ACTUAL OBSERVED CONCENTRATIONS . . .
C---
      CH4A=YOBS(1,J)*TOTCARB/100.
      C2H2A=YOBS(2,J)*TOTCARB/10C.
      IF(AMAX1(H,C,O,CH,CH2,CH3,OH,C2)/AMIN1(CH44,C2H2A).GE. 0.01)
```

THE FOLLOWING DATA WAS USED FOR ONE CASE SIMULATION.

	0 5.2E+G3	2 2,15-30	1.2E-10	2.85-33
9.35	7.2E+3	7.45-1	+ 1.2E-15	2 2521.
m ~	8.0E+02	1.0E-15	3.9E-34	1: E-32
.979	5.26E-2	7.0E-32	•0	0.
.9758	1.0E+00	4.0E-13	2.0E-12	0.
.8293	.75E+00	1.2E-30	1.95-13	ŋ.
ī	1.03E+1	8.3E-17 1.2E-30	2.1E-30	E-12 2.0E-32
1.43	1.4E+00	9.5E-17	8.8E-12	2.0E-12
.1486	0.2E+00	5.2E-35	2.5E-12	4.0E-25
2.380	0.8E+60	2. 4E-09	2. CE-10	2.8E-13

SUGGESTIONS FOR FUTURE WORK

The experimental and theoretical work reported here suggests several additional experimental programs in plasma chemistry.

Probably the easiest program to organize would be a detailed study of all the variables that enter into the kinetic modeling of the reaction system. Because of instrumentation limitations, the electron densities and plasma temperatures in this study had to be determined indirectly by theoretical approximation or by estimation based on data reported by other researchers. The electron density enters into the dissociation rates and the temperature influences the volume of gas flowing through the discharge and recombination zones, thereby influencing residence time. If the estimates of these variables are in error, some of the rate constants in the model will be in error by some constant factor, although the total model will work accurately. Therefore, a reasonable experimental project would consist of a series of experiments at specified conditions (determined from the present work to guarantee results) to simultaneously measure conversions to CH_4 and C_2H_2 , electron density, plasma temperature, plasma pressure, plasma length, plasma cross sectional area, absorbed power density, and residence time. All of this data could be analyzed with the existing model and an improved fit would almost certainly result.

This program would require an electronic or spectroscopic technique for measuring electron density and an optical, spectroscopic, or electrical technique for measuring plasma and recombination zone temperatures. It should be noted that standard devices such as thermocouple probes and optical pyrometers will be subject to possible error. This error will be due to the heat generated by recombination reactions at the surface of any object inserted into the plasma. Optical pyrometers will also be influenced by radiation emitted by the glowing tube wall. Probably the best approach would be a spectroscopic approach (based on line-broadening) or an optical pyrometry method that compensates for the inherent errors.

An additional experimental project that would provide valuable information would involve emission or absorption spectroscopy of the plasma zone to determine if intermediate hydrocarbon species do occur there.

This would require very sensitive instruments due to the extremely low concentrations of intermediates. A detailed study of the absorptions of atoms and radicals and of the effects of the high-energy environment on emissions (or absorptions) should be undertaken beforehand.

Another type of research program could involve a series of studies of the effects of different ways of mixing reactant gases. A tubular glass probe could be used to inject H_2 into a CO plasma, or to inject CO into an H_2 plasma. The same system could be used to inject gases into the region immediately downstream of the plasma. High flow rates might be desirable. A variation on this approach would be to discharge a highly dissociated CO plasma into H_2 . These studies could provide insight into the reaction mechanism. The type of gas injection might very easily influence the product distribution.

A third research program could concentrate on the effects of quenching and reactor flow patterns. Ideally, the loss of free radicals in wall recombination reactions should be minimized. This would suggest a reactor geometry where feed enters at both ends of the plasma zone, and where the products are withdrawn from the center through a quench probe. Another approach would be to devise a cavity and reactor system in which the quench system would be adjacent to the plasma zone; perhaps it could form an integral part of the end of the cavity. A quench probe with reactant gas injection within the probe, or quenching by mixing with a reactive gas could be studied.

A fourth alternative would be to investigate new types of reactions, such as degradations of large molecules to smaller ones. A system for this type of experiment would be relatively easy to set up; perhaps the only new piece of equipment would be a gas chromatograph.

Finally, it may be desirable to investigate new or alternative ways of generating a plasma, such as RF induction coils, arcs, or waveguide-type reactors. The objective would be to eliminate the geometric and electrical constraints that limit the design and location of quench systems. Reactor design could also be studied to alleviate the tube wall heating problem. Perhaps a large evacuated plasma zone with a central inward-flowing plasma and a central quench probe withdrawal point would reduce the rate of atom migration to the reactor walls.

